A study on Structural, Morphological, Dielectric and Magnetic properties of Gadolinium and Tin co-doped BiFeO$_3$ Nanoparticles

Author

Sijjal Ali Sadaqat
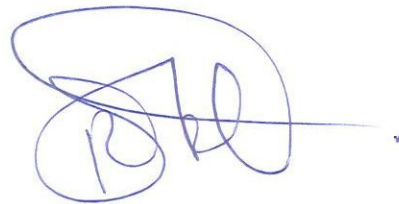
NUST201463638MSNS78114F

Supervisor

Dr. Iftikhar Hussain Gul

DEPARTMENT OF PHYSICS

SCHOOL OF NATURAL SCIENCES

NATIONAL UNIVERSITY OF SCIENCES AND TECHNOLOGY

ISLAMABAD

JUNE, 2018

National University of Sciences & Technology

MS THESIS WORK

We hereby recommend that the dissertation prepared under our supervision by: SIJJAL ALI SADAQAT, Regn No. NUST201463638MSNS78114F Titled: A Study on Structural, Morphological, Dielectric and Magnetic properties of Gadolinium and Tin co-doped BiFeO3 Nanoparticles be accepted in partial fulfillment of the requirements for the award of **MS** degree.

Examination Committee Members

1. Name: Dr. Faheem Amin _____   Signature: _____

2. Name: Dr. Zakir Hussain _____   Signature: _____

External Examiner: Dr. Muhammad Mumtaz _____   Signature: _____

Co-Supervisor: Dr. Syed Rizwan Hussain _____   Signature: _____

Supervisor's Name: Dr. Iftikhar H. Gul _____   Signature: _____

_____
Head of Department

12.06.2018
_____
Date

COUNTERSINGED

Date: 12.06.2018

_____
Dean/Principal

THESIS ACCEPTANCE CERTIFICATE

Certified that final copy of MS thesis written by **Mr. Sijjal Ali Sadaqat**, (Registration No. **NUST201463638MSNS78114F**), of **School of Natural Sciences** has been vetted by undersigned, found complete in all respects as per NUST statutes/regulations, is free of plagiarism, errors, and mistakes and is accepted as partial fulfillment for award of MS/M.Phil degree. It is further certified that necessary amendments as pointed out by GEC members and external examiner of the scholar have also been incorporated in the said thesis.

Signature: _____

Name of Supervisor: Dr. Iftikhar H. Gul

Date: 12.06.2018

Signature (HoD): _____

Date: 12.06.2018

Signature (Dean/Principal): _____

Date: 12.06.2018

Acknowledgements

Dedicated to my exceptional parents and adored siblings whose tremendous support and cooperation led me to this wonderful accomplishment

Abstract

$Bi_{1-x}Gd_xFe_{1-y}Sn_yO_3$ (BGFSO, x=0, 0.1, 0.15, 0.25; y= 0, 0.1) nanoparticles were synthesized by double solvent sol-gel method. The effects of co-doping of Gd and Sn into pure BFO on the structural and morphological properties of the prepared samples were analyzed using XRD and SEM. XRD patterns showed distorted rhombohedral structure of pure BFO which undergoes phase transition from rhombohedral to orthorhombic structure due to the Gd substitution in BFO. From SEM, clear voids and porous network can be observed and agglomeration of particles can be attributed to the addition of Gd substitutions to the BFO. The analysis of the dielectric properties of the samples exhibited the decrease in the values of dielectric constant and dielectric loss with the increase in frequency of the applied field due to dielectric relaxation phenomenon and no change in values were observed at higher frequencies. AC conductivity of the samples increased with the increments in frequency. The hysteresis behavior was revealed for different concentrations of magnetically active Gd added in BFO host, increments in the concentration of Gd resulted in enhanced saturation magnetizations for different samples mainly due to the alteration in antiferromagnetic ordering at the particle's surface, phase transition due to the Gd substitution, collapse of space modulated spin, suppression of oxygen vacancies and increase in number of Fe ions.

Table of Contents

List of Figures:

CHAPTER 1: INTRODUCTION AND LITERATURE REVIEW

1.1 Nanotechnology

The science of materials that are between 10^{-9} and 10^{-7} of a meter in size, is known as Nanotechnology [1]. The word "Nano" is originally a Latin word, it means "dwarf". One thousand millionth of a meter is an ideal range that nanotechnology offers. It can also be defined as the science of devices and materials that exhibit novel and changed chemical, physical and biological phenomenon due to their extremely small size that is in nanoscale range. This branch of science, Nanotechnology, deals with the phenomena that occur at nanoscale very close to atomic or molecular level. As the size of materials reduce to nanoscale, the principles of quantum mechanics become more important as compared to the classical mechanics which is used for the explanation of various phenomena that occur in bulk materials. As the principles of classical mechanic's flop that very small level, quantum mechanics has been proven worthy to demonstrate the behaviour of materials at nanoscale [2]. At the size of about 10^{-9} of a meter, the quantum effects are enhanced, which results in enhanced surface to volume ratio or very large surface area [3].

A well scientist, Richard Feynman introduced the concept of nanotechnology. He has a very famous saying, "there is plenty of room at the bottom", in favour of the idea of advancement in the field of materials and devices that fall in nano or atomic scale [4].

1.2 Nanoparticles

The particles that have at least one physical dimension in the nanoscale (from 0 to 100nm) are known as nanoparticles. The physical properties of the materials change when they are reduced to nano size, their properties such as physical, chemical, optical, magnetic are changed from what they show when they are in bulk. The nanoparticles have multiple importance in the fields of electronics, cosmetics, magnetic, pharmaceuticals, biomedical and optoelectronics [5].

1.3 Classification of Nanoparticles

The nanoparticles are can be categorised in a total of four classifications on the basis of the degrees of freedom they possess.

- Zero dimensional nanoparticles.
- One dimensional nanoparticles.
- Two dimensional nanoparticles.

- Three dimensional nanoparticles.
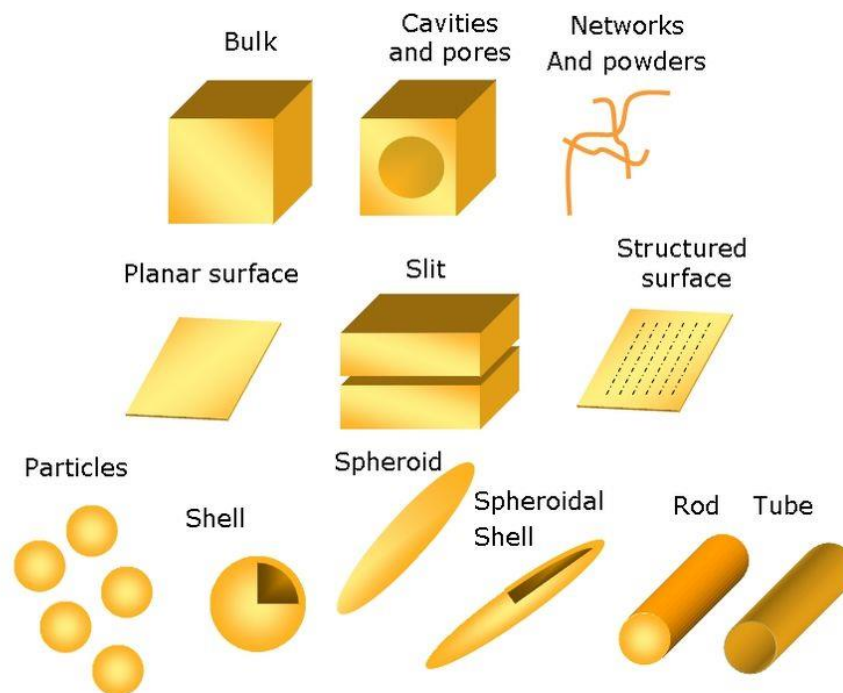
Fig 1.3: Classification of nanoparticles [6].

1.3.1 Zero dimensional nanoparticles

The limitation of three dimensions within the nanoscale range gives rise to the zero-dimensional nanoparticles. Quantum dot, nanorings, nanoshells are the examples of zero dimensional nanoparticles.

1.3.2 One dimensional nanoparticles

The material is which degree of freedom is limited to two dimensions except one are known as one dimensional nanoparticles. It means that electron can move in one dimension but not in other dimensions. One dimensional nanoparticles include nanowires, nanotubes, nanorods and naofibres.

1.3.3 Two dimensional nanoparticles

The material is which degree of freedom is limited to one dimensions except one are known as two dimensional nanoparticles. It means that electron can move in two dimensions but restricted in the third. Nanofilms, nanolayers and nanocoatings are the examples of two dimensional nanoparticles.

1.3.4   Three dimensional nanoparticles

These are also known as the bulk nanoparticles. Group of nanowires, nanotubes as well as the clusters of nanostructures or nanoparticles that exist is clusters are the examples of three dimensional nanoparticles. They have all three dimensions in macroscopic range and have all three degrees of freedoms. Although they are not entirely in nano range but they exhibit novel, fascinating and distinctively extraordinary properties because of the fact that they are comprised of nanoparticles with novel properties.

1.4   Parameters of interest

The drastic change in the properties of materials occurs when their size in reduced to nanoscale. Following are the parameters that are responsible for the change in properties that can be witnessed at nanoscale.

- Physical properties:
1. Size, aspect ratio, surface area, shape of the nanoparticles.
2. Structural defects and crystalline structure of materials.
3. A kind of size distribution, nanoparticles possess.
4. Morphology.
5. Agglomeration of particles or its aggregation rate.
6. Solubility, that a certain material offers.
- Chemical properties:
1. Parameters like structural formula or the molecular structure of the nanoparticles.
2. The chemical composition of the nanoparticles as well as the level of purity it achieves.
3. One of the important parameter is the phase identity.
4. Surface chemistry that includes reactive sites, charge, tension, zeta potential and more.

The reduction in the size of the material results in the properties that are different and quite unique to the properties that they exhibit in bulk state. There are number of phenomena that can be the cause of the change in the properties of nanoparticles. Following are the possible phenomena that influence the properties of matter at nanoscale.

- o   Quantum confinement.
- o   Enhanced surface energy.
- o   Large number of atoms that are available on the surface of the particles.
- o   Less gravitational force experienced by the particles at nanoscale.

1.5   Properties of Nanomaterials

Following are the physical properties of nanomaterials which they exhibit when they are reduced to nano scale which dramatically differs from the properties they exhibit in their bulk state.

1.5.1   Electrical properties

The properties of nanoparticles which are related to the electrical conductivity or resistivity are termed as electrical properties of nanoparticles. There are various techniques which are used for the analysis of the electrical properties of nanoparticles. As we reduce the size to nano scale the material exhibits quite dramatic changes. The reduction of the particle size changes the electrical resistance and makes its value quite large, and this is because of the fact the number of electron wave modes which participate in the process of conduction of the charges get smaller by quantised steps. However metallic nanomaterials exhibit decreased in conductivity, When the size of these particles/materials is reduced so the interesting thing is the conducting nanomaterials behave as non-conducting below certain critical size and temperature.

1.5.2   Optical properties

Scientists have found fascinating properties of nanomaterials in the field of optics that have great importance and these properties are providing the gateways for opportunities to use nanoparticles in some of the very useful applications which are related to optics.

Following are the fields in which the optical properties of nanomaterials have great importance.

- Solar cells
- Optical sensors
- Bio-Medicine
- Laser
- Photocatalysis

The optical properties of the nano particles are dependent on the fabrication route and the physical properties like size, shape, surface and the amount of doping.

1.5.3   Magnetic properties

The magnetic properties of nanomaterials are detected on the basis of the physical dimensions which these particles possess. The different properties of nanoparticles can be ascribed in the following fields.

- Medical engineering

- Information storage media
- Magnetic sensors
- Spintronic devices

The ferrites are one of the most researched magnetic nanoparticles. The material which is fabricated and explored in this research is also a ferrite, Bismuth ferrite (BFO). It is multiferroic having transition temperature 1103kelvin approx. The exhibition of ferromagnetic behaviour is one of the famous phenomenon in the field of multiferroics, which is caused by the moments from the central spin structures.

1.6   Applications of nanomaterials

There are various fields in which nanomaterials have great importance, they have numerous applications in the modern technology such as

- Medicine
- Fuel cells
- Food industry
- Agriculture
- Electronics

Some of the applications of multiferroic materials are as follows

- Digital recording
- Magnetic sensors
- Spintronic devices

1.6.1   Fuel cells

The device that is used to transform chemical energy from fuel (anode) and oxidant (cathode) to electrical energy. Electrodes play the most important role for the fuel cells to function. Following are two methods which can be optimised

- By changing the structure of fuel cells
- By using active catalysts

In order to enhance conductivity and gas transport of the fuel cells there's a need to clean the surface area of the electrodes which play an important role in fuel cells also the surface area of eletrodes have to have enough maximum contact area for the catalyst electrolyte and reactant gases.

1.6.1.1 Microbial fuel cells

In this type of fuel cells, some bacteria are used for the production of electrical energy. By consuming wastes which are soluble in water for example sugar, alcohol and starch. This

property is very helpful in converting the energy from the waste into the electrical energy. This is a kind of technology in which we use the chemical energy stored in the industrial or domestic waste is converted to electricity. For the conduction of electricity charged particles are transferred towards the anode from bacteria. In the water waste, there's a kind of energy known as chemical energy which is stored in the organic molecules and this energy is released when the organic molecules are broken down such as carbon dioxide. Carbon nanotubes can be used for cell growth electrodes of microbial fuel cells. Because of the fact that the carbon nanotubes have very good mechanical properties as well as a very large surface area. This huge surface area of the electrodes and the three-dimensional cell growth will take part in growth of bacteria and as the result bacteria gets immobilised. A large number of bacteria can be grown on a large surface area of the carbon nanotubes and these bacteria produces hydrogen.
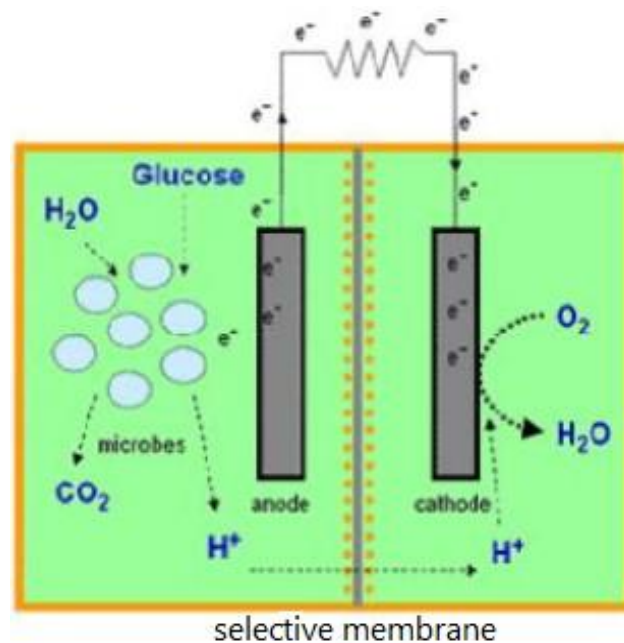
Figure 1.6.1(a): Block diagram of Microbial Fuel Cell

1.6.1.2 Solar cell

A solar cell also known as photovoltaic cell is a device that is used to convert photons into electricity. Nano hybrid materials have been used for the synthesis of solar cells which exhibit improved extinction coefficient photosensitization properties and the work efficiency. So far there's a huge amount of research work going on for the production of inexpensive, stable and tuneable band gap solar cells.

6

Basically, the solar cell is produced to fulfil two functions.

- Photogeneration of charged particles
- Separating the charged carriers to a contact which is conductive to produce electricity

We can arrange the solar cells into large arrays thousands of cells make a single array and they can function as a unit to produce electrical power means they work as electric power stations that converts the light from sun into electricity that can be used in industries, homes etc.
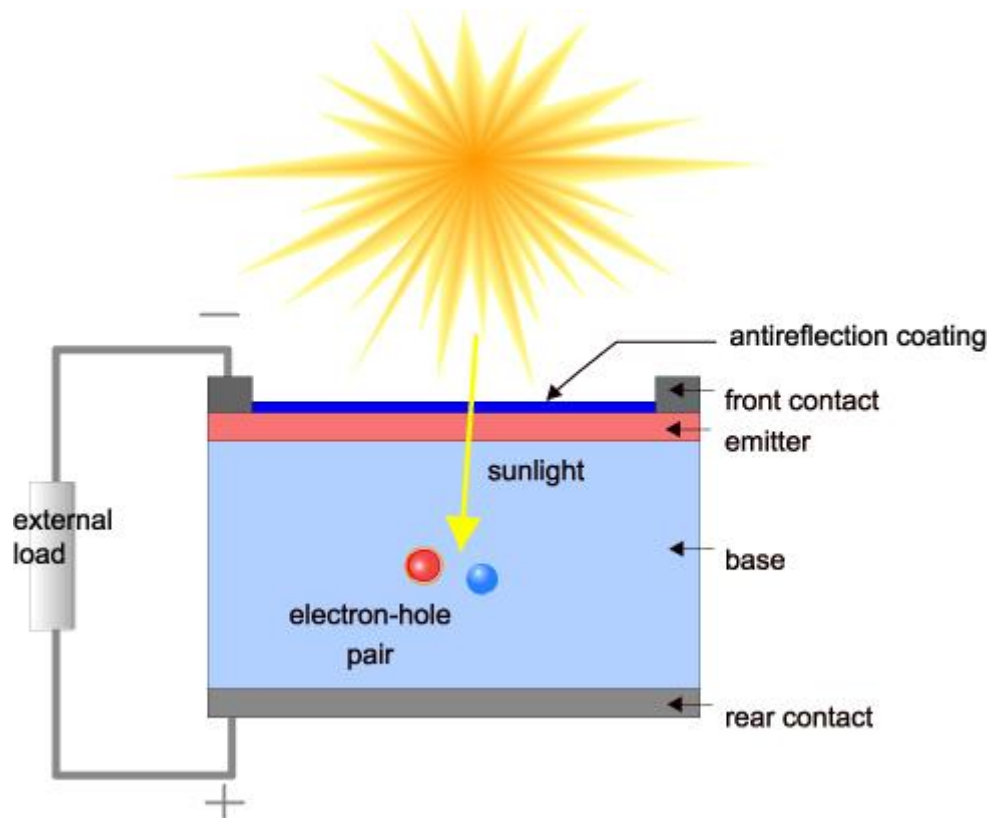
Figure 1.6.1: (b) Solar cell.

1.6.2 Catalyst

Nanomaterials have a very large surface area and due to this exceptional property, they exhibit unique surface activity and make them a perfect candidate to be used as a nano catalyst. Nano crystalline aluminium is used as a solid fuel that is used in rockets because of the fact that it has a high reaction rate but the aluminium in bulk is used to manufacture utensils so the nano crystalline aluminium can be used to send the load wage in space because of its highly reactive nature. The surface activities of the nanomaterials are responsible for their use as catalysts.

Figure 1.6.2: Catalysis.

1.6.3 Television displays

The pixel size of the digital display units such as computer's monitors is responsible for the resolution of Television. Normally these pixels are composed by phosphorous. This material has the property to light up when hit by an electron which is coming from cathode ray tube (CRT). The nano crystalline materials such as cadmium sulphite lead telluride and zinc sulphite are the reasonable candidates which can be used to improve the resolution because they can enhance the performance of the displays as they offer smaller pixel sizes. Sol-gel method is used for the preparation of these nano crystalline materials there is another aspect which is that the nano phosphorous is more inexpensive than the phosphorous in bulk. So, it greatly reduces the cost of these screens which offer high definition displays.

1.7 Ferrites

The oxides of iron with different metals are known as ferrites [7-9]. The classification of ferrites is dependent on combination of metals, stoichiometry and the crystalline structure they possess. These are the factors that influence the magnetic and electrical properties of the ferrites. Ferrites were fabricated in Tokyo, Japan for the first time in the history. They exhibited

the properties of hard magnetic at that time, later they were used for other applications according to their properties and use in specific field. The crystalline structure of the ferrites actually determines their magnetic properties. Following are the classes of ferrites according to the crystal structure.

- **Spinel ferrite**

The name of this class of ferrites is after the $MgAl_2O_4$ mineral. Spinel ferrites contain 2 iron atoms, 4 oxygen atoms and 1 metal atom. These are the materials that can be easily magnetised as well as demagnetised [10,11]. It has the general formula AB_2O_4, A is to represent metal ion, B is for iron ion, and O represents the oxygen atom. The crystal structure of the spinel ferrite is shown in the figure.
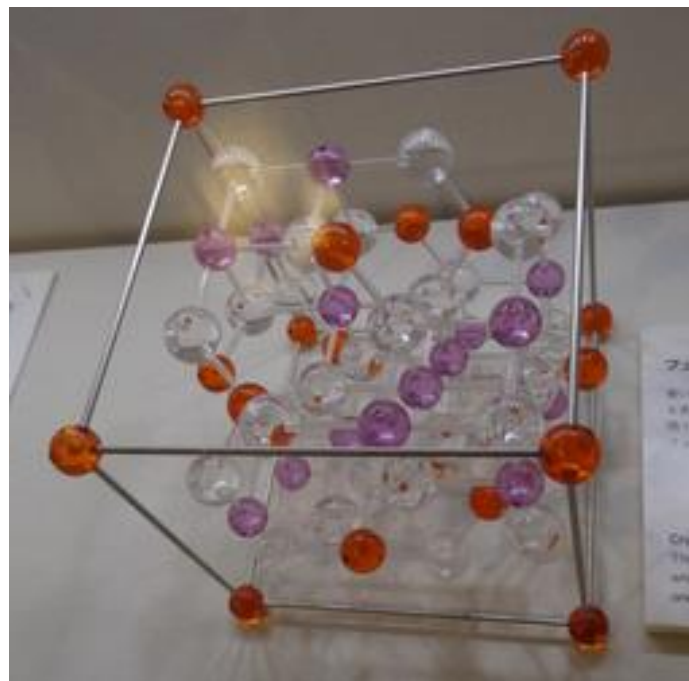
Fig 1.7(a): Crystal structure of Spinel ferrite [12].

- **Hexaferrite**

The type of ferrites that possess hexagonal crystal structure are called hexaferrite. They behave like hard magnets as they have large value of coercivity that makes it difficult to magnetise or demagnetise. Crystal structure is shown in the figure.
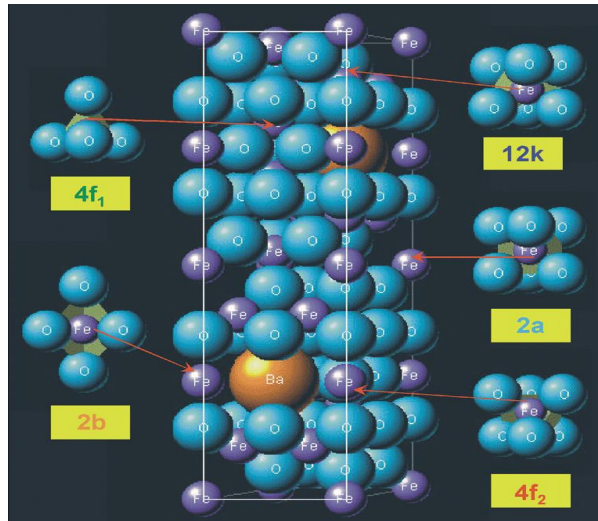
Fig 1.7(b): Hexaferrite crystal structure [13].

So, most of their applications are as permanent magnets. They have a relatively complex crystalline structure as compared to the other ferrites. It is comprised of different parts and layers. It consists of two hexagonal sites and other sites are tetragonal and octagonal. Permanent magnetic property of these ferrites is due to this kind of anisotropy.

1.8 Classification of Ferroics

- Ferroelectric materials
- Antiferroelectric materials.
- Ferroelastic materials.
- Ferrotoroidic materials.
- Ferrimagnetic materials.
- Antiferromagnetic materials.

1.8.1 Ferroelectric materials

These materials exhibit spontaneous stable polarisation, when the external electric field is applied, this polarisation switches hysterically. Ferroelectric materials possess piezoelectric properties. Whenever the external load is applied, the electric charge is produced that is proportional to the amount of external applied voltage and the deformation is produced which is proportional to external voltage that is applied.

1.8.2 Antiferroelectric materials

These materials exhibit antiferromagnetism, this means that the magnetic moments inside the materials possess the alignment of in opposite direction relative to direction of neighbouring magnetic moments of the atoms. There is a kind of ordered dipole moment that

cancels the effects of other moments and the net moment becomes zero within each unit cell of the material. That is the behaviour they show at relatively low temperature. And this tend to vanish at values of temperature above certain point. The temperature at this point is known as Neel temperature.

1.8.3 Ferroelastic materials

The exhibition of the deformation whenever the stress is applied which is also proportion to the stress applied is known as Ferroelasticity. So, there is actually an induction of the strain that result in the phase change of material which may be another stable phase with different crystal structure or with different orientation so, in short, these materials exhibit a spontaneous deformation, when the stress is applied. This stables spontaneous switches hysterically if the external stress provided.

1.8.4 Ferrotoroidic material

multipole expansion referred to the expansion of electromagnetic fields along with electric and magnetic multipoles. Some addition terms come into effect in electrodynamic multipole expansion. And the origin of toroidal moment is the coefficient of those terms that arise during the expansion. Two types of toroidal dipoles are revealed, axial toroidal dipole that exhibit the arrangement of toroidal charge and the polar toroidal dipole that represents the field created by a solenoid. The order parameter is shown by these materials that is very sable and spontaneous, and magnetization or polarisation is the cause of this order parameter.

1.8.5 Ferrimagnetic materials

The magnetic moments that are created inside the material do not cancel each other entirely and there exist a net magnetisation that is exhibited by the material unlike the antiferromagnetic materials. This net magnetisation can be changed by changing the values of external magnetic field.

1.8.6 Antiferromagnetic material

In these materials, the behaviour of adjacent ions is like tiny magnets. Throughout the materials these tiny magnets align themselves into antiparallel arrangements, as they cancel each other effects so the net magnetisation is zero. The opposite and antiparallel alignment of the magnetic atoms and ions present in these materials cancels the magnetic moments that are produced in these materials.

One of the characteristic of each antiferromagnetic material is that at above certain temperature, this spontaneous opposite and antiparallel coupling disappears, that temperature is known as Neel temperature. Some of the antiferromagnetic materials have shown Neel temperature that is about few hundred degrees above the room temperature.

Special behaviour can be observed in antiferromagnetic material by changing the temperature while applying magnetic field. No or zero response is shown by the material at low temperature because of the maintenance of the antiparallel arrangement of the magnetic atoms. But at relatively higher temperature, this coupling is disrupted and the material show some response against the magnetic field. The weak magnetisation can be observed as long as the temperature is below Neel temperature, the antiparallel ordering is disturbed due to thermal agitation which is resulted from the increase in temperature above certain level.

1.9   Multiferroic materials

The term Multiferroic refers to the materials that simultaneously exhibit at least two of the effects of ferroic properties like ferromagnetism, ferroelectricity and ferroelasticity. These materials have a variety of applications in the field of information storage, optoelectronic devices and transducers [14,15]. The group of rare earth ferrites, perovskite metal oxides as well as magnetites contains various multiferroic materials. The unusual magnetic structures in multiferroic materials give rise to ferroelectric polarization [16,17]. The presence of the cyclic variants in the orientation of various magnetic moments induces electric polarization [18,19].
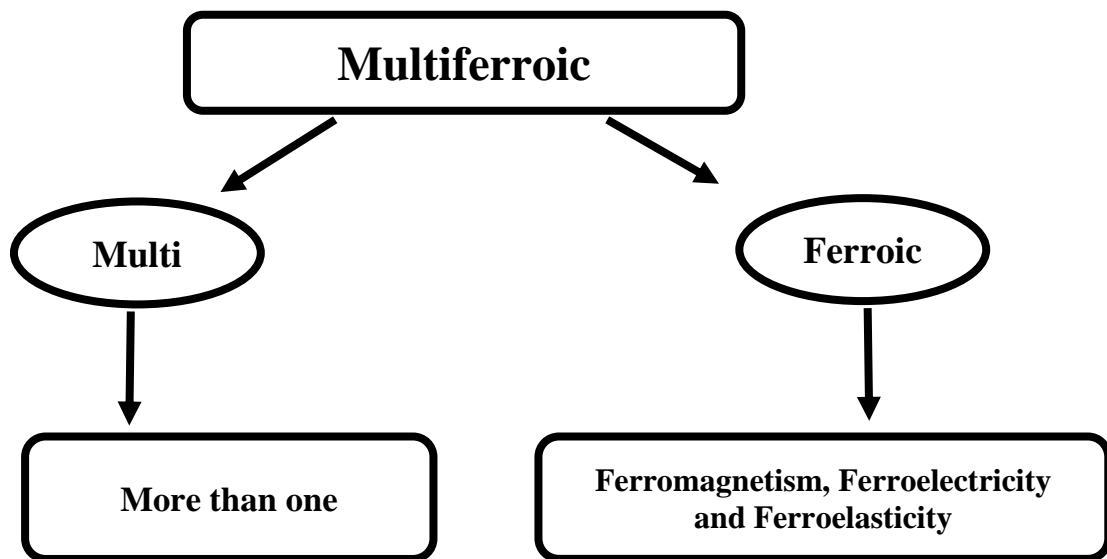
Fig 1.9: Multiferroic

1.10   Types of Multiferroic materials

Following are the two types of multiferroic materials.

- Type 1 multiferroic materials.
- Type 2 multiferroic materials.

1.10.1 Type 1 multiferroic materials

These are the materials in which the sources of ferroelectricity and magnetism are different and seem to be independent of each other but there exist a kind of "coupling" that is present between them. The coupling which is present between ferroelectricity and magnetism, exhibited by the materials, is weak. The subclasses of these materials are as under.

- Multiferroics that have perovskite structure.
- Multiferroic in which ferroelectricity is due to lone pairs [20].
- Multiferroics that exhibit ferroelectricity because of the charge ordering in them.
- Geometrically frustrated multiferroics.

1.10.2 Type 2 multiferroic materials

These materials exhibit very strong magnetoelectric coupling. The magnetically ordered state are responsible for the occurrence of ferroelectricity in these types of multiferroic materials. There is a particular type of magnetism that is present in these types of multiferroic materials and this magnetism is the cause of ferroelectricity exhibited by these materials since the discovery of type 2 multiferroic materials.
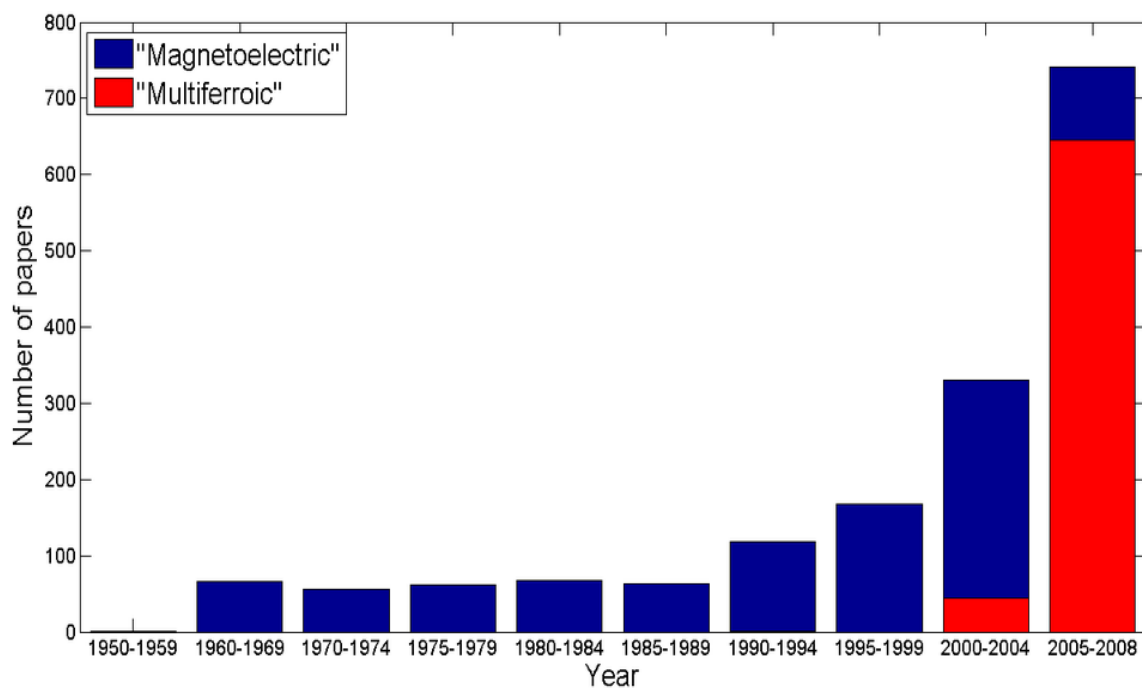
Fig 1.10: Multiferroics history use of terms magnetoelectric and multiferroic [21].

1.11 Literature Review

1.11.1 BFO and Doped BFO

Bismuth ferrite ($BiFeO_3$, BFO) is a multiferroic, exhibits ferroelectricity and G-type antiferromagnetic ordering simultaneously at room temperature [22,23]. BFO has a distorted rhombohedral perovskite structure having high curie point (T_C = 1103 K) and a Neel point (T_N =643K) [24,25,26]. The exhibition of the weak magnetization at the room temperature is due to the residual spin that results from a modulated cycloid spin structure of BFO having a periodicity of 62 nm [27]. BFO, a room temperature multiferroic has application in various fields like information storage, spintronics, sensors, photocatalyst and actuators, etc [28]. it is unfortunate that issues like weak macroscopic magnetism and leakage problems that result from the poor quality of the sample like existence of oxygen vacancies and nonstoichmetry have restricted its applications. The number of methods have been used for the fabrication of BFO particles having pure phase since 1960. These methods include sol gel [29, 30], co-precipitation, hydrothermal [31-33], sonochemical [34], and microwave-hydrothermal, molten salt synthesis [35]. Various impurity phases, like $Bi_2Fe_4O_9$ and $Bi_{25}FeO_{39}$ are formed during the preparation are the main obstacles in the path leads to the preparation of pure phase BFO particle or thin films. Pure and doped BFO has been synthesized by using wet chemistry routes that revealed unique advantages like getting homogeneous solution of metal ions, trouble-free and controllable reactions, obtaining samples that with regular and uniform morphology and dimensions.

Recent studies show that researchers have been trying to improve the structure and the physical properties of BFO by substituting many elements in BFO. BFO doped with Gd [36], La [37], Mn [38, 39], Co [40], Ho [41], also co-doping with La-Co [42], La-Mn [43], (La,Pr)-Co[44] is supposed to have a positive impact on the reduction of impurity phases and enhancement of electrical and magnetic properties. Lattice distortion that result from doping of Gd which has large effective magnetic moment and smaller ionic radius as compared to the Bi ions, can significantly enhance the magnetization [36]. Mn doped at Fe-site can enhance the ferroelectricity by reducing the leakage current density and oxygen ion vacancies [45-47]. In this work, Gd and Sn were chosen to substitute Bi and Fe in pure BFO, respectively. $Bi_{1-x}Gd_xFe_{1-y}Sn_yO_3$ (BGFSO, x=0, 0.1, 0.15, 0.25; y= 0, 0.1) were synthesized by double solvent

sol-gel method. The structural, morphological, electrical and magnetic properties of the as prepared samples were explored.

Instabilities is the pressure were analyzed by Haumont. The infrared spectroscopy and the diffraction analysis revealed that the transition of phase of BFO occurred at around 3 and 10 GPa. The displacement of the small cations as well as the octahedral tilts were found in monoclinic space groups. With the increase in pressure the suppression of polar character of the BFO occurs above 10GPa due to the displacement of cations [48].

The single crystal of BFO is prepared in highly purified form by using flux method. At room temperature, BFO exhibited ferroelectric behavior and showed ferroelectric hysteresis loop at room temperature. The solid solution of BFO with another perovskites structure material (BFO-Pb(Ti,Zr)O_3 is formed in order to increase dielectric constant and decrease dielectric loss. The epitaxial thin film undergoes a structural change that caused the increase in polarization [49].

The synthesis of BFO thin films by the use of dip coating technique was reported by scientists. Thin film was deposited on the substrate, the variations in the chemistry of the solution is responsible to change the properties of thin film. The change in viscosity of the solution deeply influenced the thickness of the thin film and in this way the thickness of thin film was controlled [50]. Also, a report says about the existence of the couple of magnons, and the analogy can be made between these magnons and the spin wave excitations in and out of the cycloidal plane [51].

Scientists reported that at curie temperatures Tc between 820-830 °C the phase transition occurs from R3c space group to orthorhombic phase along with the transition from ferroelectric to paraelectric. The nature of the transition from rhombohedral to the orthorhombic in BaTiO$_3$ is different from the same transitions in NaNbO$_3$ [52]. Furthermore, the piezoresponse as well as the polarized neutrons scattering by characterization of the single crystal BFO using AFM. He reported that the single crystal of Bismuth Ferrite showed one ferroelectric domain the polarization directions are distinctive below the curie temperature[53].

Moreover, the fabrication of BFO by Sol-gel method. Bismuth nitrate and iron nitrate were used in this method for preparing pure BFO. The samples were sintered at 600^{0}C. The particles, obtained by this method, were 200nm in size [54]. Another study reported the applications of BFO nanoparticles in microelectronics, optical coating and sensor technology, as they exhibited very high ionic conductivity and it is a good candidate to be used as an electrolyte material to be consumed in fuel cell as well. There is another study, in which the solution evaporation method is used for the fabrication of Bismuth ferrite nanoparticles [55].

In another study, solid-state reactions were used for the synthesis of multiferroic (1-x) $BiFeO_3$ – $xPbTiO_3$. The existence of morphotropic phase around the boundary region is revealed by the analysis XRD patterns for this system. In the boundary region, simultaneous existence of rhombohedral, tetragonal and orthorhombic phases is reported. The change in the temperatures, that is responsible for the antiferromagnetic ordering, is observed and it was attributed to the various structural effects that influenced the magnetic interactions between the rhombohedral and tetragonal phases [56].

Chapter 2: Synthesis Technique of Nanoparticles

2.1 Introduction

Developing novel materials with enhanced properties, better functionality with effective cost is the prime concern for material scientists. So, there is a need to find better ways to synthesise materials that show better performance. There are various methods that have been developed to produce nanomaterials that display improved properties and these methods allow to have a better control over the particle size distribution [57].

Following are two approaches to the fabrication of nanomaterials.

- Top down approach.
- Bottom up approach.

2.1.1 Top down approach

Using this approach, we start with the bulk material and make it smaller and smaller, in this way the larger particles of the material are broken down by the use of physical processes like crushing, grinding or milling. Normally this is not a suitable route if there is a need to prepare samples with uniform distribution. As it is very hard to control the size of the particle at nano scale. There is another problem with the top down approach is that it leads to surface imperfections. These imperfections significantly affect the physical and chemical properties of nanostructures and nanomaterials. It is also well known that this conventional approach is the cause of crystallographic damage to the material being synthesised for example using top down lithography technique can cause crystallographic damage and it can also introduce defects during the process while etching.

2.1.2 Bottom up approach

In this technique nanomaterials are synthesised by assembling the atomic or molecular precursors until the formation of desired structures. In other words, nanostructures are formed atom-by-atom or molecule-by-molecule. The nano materials that are obtained by using this technique by using this technique exhibit a uniform size distribution and shape. This method also provides more control during the reactions to synthesise desired materials.

It has always been a great challenge to develop eco-friendly and expensive processes to synthesise nanoparticles with better size distribution, morphology, quantity and quality [58].
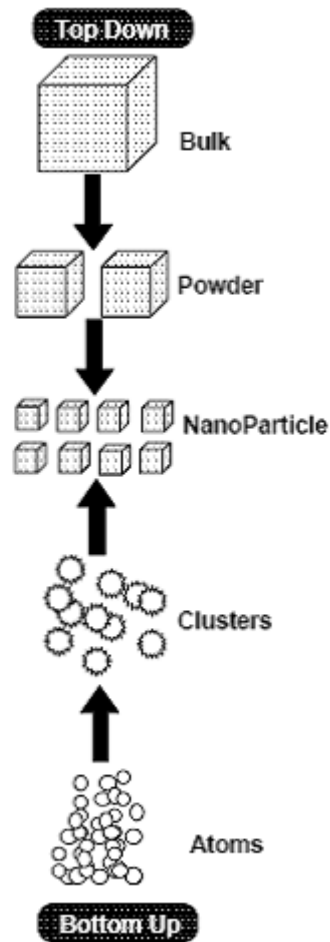
Fig 2.1: Schematic of top down and bottom up Approaches [59].

2.2   Sol-gel technique

The methods of crystal growth include,

- Molecular beam epitaxy (MBE)
- Chemical vapour deposition (CVD)
- Sputtering
- Chemical bath deposition (CBD).
- Sol gel Method [60-63].
- Citrate gel method [64]
- Micro Emulsion Technique [65].
- Ferrioxalate precursor method [66].

Sol-gel process is one of the most commonly used technique for the fabrication of Nanoparticles in the fields of ceramic in engineering and material science. In this research work, the technique used for the synthesis of BFO nano particles is also sol-gel.

This technique is typically used for the fabrication of metal oxides. In the process of fabricating nanoparticles using this technique, colloidal solution which is known as (sol) acts as a precursor for the network of discrete particles or polymers (gel). Metal salts and alkoxides that serve as a typical precursor and they undergo different forms of Poly condensation and hydrolysis reactions.

The gradual evolution of the solution or sol to a gel-like diphasic kind of system that contains both liquid and solid phase. The change in the morphology of the solution (sol) can produce discrete particles as well as continuous polymer networks. Gel-like properties can only be recognised after the removal of significant amount of fluid in order to compensate a very low particle density in the case of colloid. There are number of ways to accomplish this, one of the simplest is that, time should be given for the sedimentation to occur and then the solution left is pour off or the method of centrifugation can also be used for the acceleration of phase separation process.
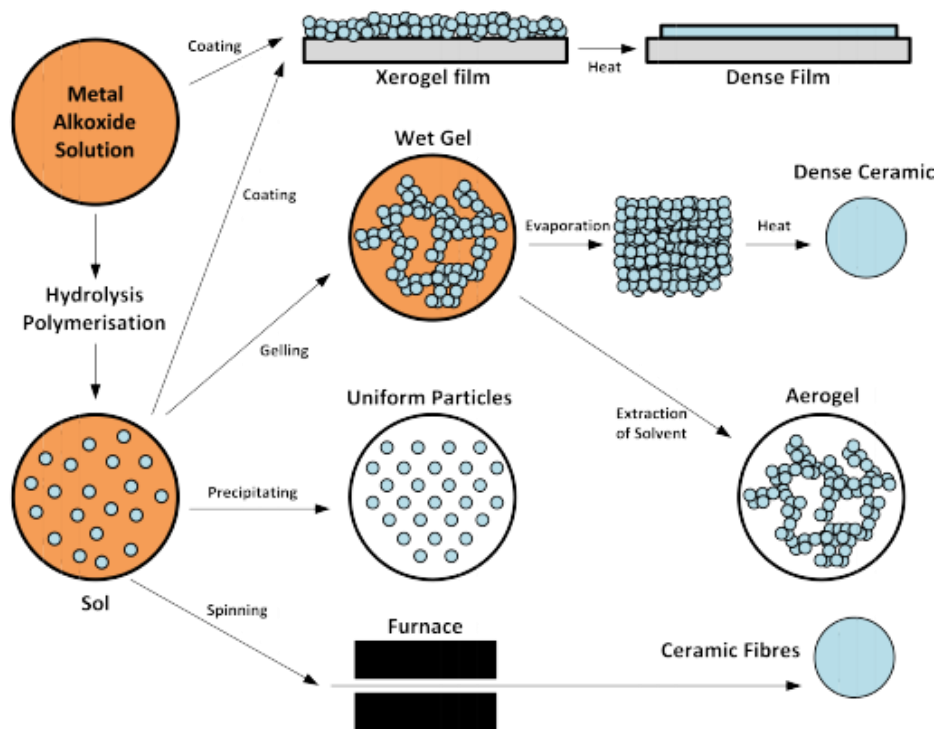
Fig 2.2: Schematic Diagram of Sol-gel process [67].

Then there comes a phase of removing the remaining liquid, and for that a drying process is required that triggers the shrinkage as well as densification. The determination of the rate of removal of the solvent is by the type of gel and the distribution level in it. The samples being prepared undergo a variety of changes that actually influence the nanostructure of the final product.

After that there comes a heat treatment phase or sintering, which is very crucial for further favourable polycondensation as well as the enhancement of the mechanical properties and promotes structural stability by the use of sintering and densification. One very useful advantage of using this technique over the others is that much lower temperature is required for the densification of the material.

The use of sol-gel technique for the fabrication of nanoparticles started in mid 1800s when it was observed that the hydrolysis phase of TEOS can produced silicon oxide in fibrous form under acidic conditions. More than 35000 publications worldwide on the sol-gel process proves that the research on sol-gel became very important in 1900s [68-72].

2.2.1 Four stages of sol-gel process
- o Hydrolysis
- o Condensation
- o Growth of the particles
- o Agglomeration of the particles
- **Hydrolysis**

  During this process, water that is added replaces the [OR] group with [OH] group. Some catalyst may be used to trigger hydrolysis. The complete replacement of the alkoxyl groups with the hydoxyl group marks the end of the hydrolysis.

- **Condensation**

  Water or the alcohol are responsible for the condensation reaction as they initiate polymerisation in order to form silocane bonds.

- **Growth and agglomeration**

  Polymerization results in the formation of siloxane bond and these bonds increase in numbers. Due to the increase in the number of these bonds, the molecules start to aggregate in the colloidal solution and the network is formed, afterwards heat treatment results in the

formation of gel. Finally, with the help of centrifugation, water and alcohol are removed from the solution and the entire network shrinks.

2.2.2   Methods of producing gel

There is a total of four ways that can be used to produce gel in sol-gel process.

1. The use of precipitating fluids and salts flocculation of colloids.
2. Gel can be produced by causing some colloidal solutions to evaporate.
3. Some chemical reactions can also be used for the production of gel that cause the shape of lyophilic molecules to change.
4. Colloids are placed with suitable fluid results in the swelling and the gel produced by this method is known as xerogel.
    The high porosity gels can be obtained by drying a wet gel at supercritical temperature in an autoclave [73,74].

2.2.3   Properties of gel

Following are the properties of gel

1. Swelling
2. Syneresis
3. Ageing
4. Rheological.

-   **Swelling**

    Fluids that helps the xerogel to solvate can give rise to swelling if the gel is placed in contact with the fluid.

-   **Syneresis**

    The spontaneous contraction of the gel give rise to syneresis followed by a discharge of gas from the liquid medium.

-   **Ageing**

    When the rate of aggregation becomes low, ageing occurs. This phenomenon results in the formation of the denser network of the gel which is denser.

- **Rheological properties**
- These are revealed when the gel starts to exhibit properties of solids such as tensile strength, elasticity, and rigidity.

2.2.4   Applications of sol-gel

1. Protective coatings

The products derived from sol-gel have numerous applications [75-80]. Thin films have one of the largest application areas, protective coating as well as decorative coatings and electro optic components can be produced by methods like spin coating and applied to metal, glass and other kinds of substrates with an aid of these methods.

2. Thin films and fibres

In the field of thermal insulation and fibre optic sensors, the proper adjustment of sol leads to the preparation of such ceramics that can result in some very fine fiber optic sensors and thermal insulation tools. There are multiple ceramic materials that are useful in various forms from bulk to nanoscale like thin films, various types of coatings and multiple fibres [81,82].

3. Nanoscale powders

Sol-gel method is used to make a variety of nanoscale powders such as zeolite, powder abrasives, that are used in the various finishing processes, and many more metal and metal oxides.

2.2.5   Advantages of using sol-gel method

Following are the advantages of sol-gel method over the other techniques that are being used to produce nanostructures [83,84].

- The synthesis of high purity materials can be achieved by using synthetic chemicals.
- The production of the homogeneous material is always very desirable and it is made possible by this technique as it uses liquid precursors with low viscosity so mixing of such solutions promotes homogenisation at molecular scale.
- One of the advantages of this technique is the occurring of the chemical reaction at low temperatures relatively because all the precursors get well mixed at the molecular level that leads to the formation of gel.

- This technique gives the power of controlling the physical characteristics like pore size and distribution.
- The achievement of the incorporation of the multiple constituents in one step.
- One can manage the production of the various physical forms of the specimen.

Some other routes for producing nanomaterials

2.3   Chemical vapour deposition (CVD)

Chemical vapour deposition is the fabrication technique used to fabricate nanomaterials especially thin films that are high-performance and high-purity. Some of the key steps included in the CVD process are as under.
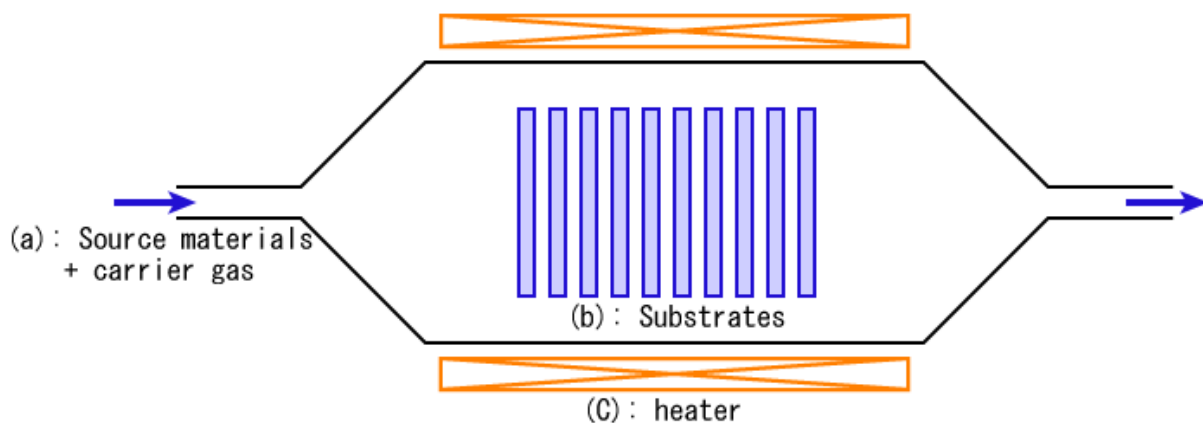
Fig 2.3: Schematic of CVD process [85].

- o   The exposition of the substrate to the precursors that are volatile.
- o   The process involves the reaction or the decomposition of the surface of the substrate by the volatile precursors.
- o   The products that are produced, are removed by the use of gas flow that removes it through the chamber in which the reaction is taking place.
- o   There are some factors on which the quality and the performance of the deposited materials depends such as reaction rate, temperature, and the concentration of the precursors used in the reaction [86].
- o   This method is very useful in obtaining nano films that are uniformly coated.
- o   The requirement of a very high temperatures above 900 degrees centigrade, is one of the limitation of this process also it is a difficult task to even scale up the temperatures [87].

- o If the activation of the reaction is by plasma, then the process in known as plasma CVD.
- o In CVD, if the reaction is activated by the use of ultraviolet radiations that are used to break the chemical bonds in the reactants then the process in known as photo-laser chemical vapour deposition.

2.4 Hydrothermal method

- In this method, a pressurised vessel known as an autoclave is used for the fabrication of the nanostructures.
- Reaction is carried out in aqueous precursor solutions.
- Inside the autoclave the temperature reaches above the boiling point of water.
- The pressure is raised to the vapour saturation.
- It is widely used for controlling grain size, morphology, crystalline structure, temperature pressure, properties of the solvent and ageing time [88].
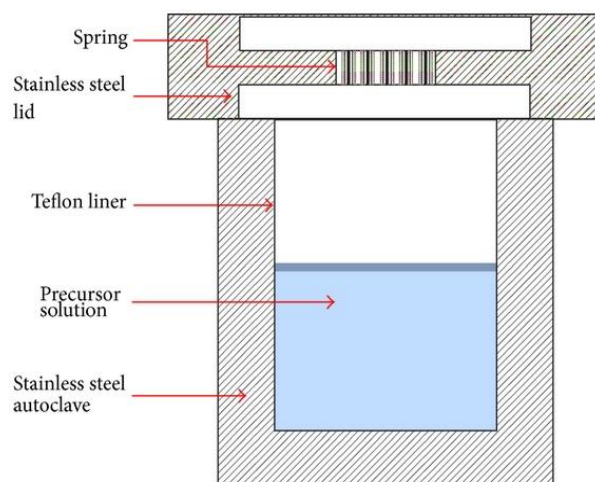
Fig 2.4: Autoclave for Hydrothermal Synthesis [89].

This method can be used for the production of different materials using physical and chemical processes in a closed system with an aid of the solutions at high temperatures and pressures. As it is the property of the aqueous solutions as well as water that they dilute at temperatures greater than 500^0C and pressures (greater than 10-80 MPa) those substances that are insoluble practically under normal conditions such as oxides, sulphides and silicates. Following are the parameters that are responsible for the kinetics and the characteristics of the products include the initial value of the ph of the aqueous solution, temperature and pressure of the reaction as well as the time taken by the reaction for completion. And for this purpose, such autoclaves are required that are made up of steel and have the ability to withstand high pressures and

temperatures for a long period of time. By the help of this method some of the additional factors that can be controlled during the fabrication process.

Moreover, this technique provides facilitation in issues such as energy saving, getting rid of equipment that use large volume, avoiding pollution, higher reaction rates, controlling the shape and nucleation. Production of the particle with better purity, better quality and better crystallinity and controlled chemical and physical properties can be achieved by the use of hydrothermal technique and this fact gives an edge to this technique over the conventional methods. The advantages of using hydrothermal method are as follows.

- The coat on the energy can be saved as the nanoparticles can be fabricated without the need of different heat treatment processes at high temperature like calcination.
- Due to the synthesis in high-temperature and high-pressure environment, the products are homogeneous which ensure the ease of controlling size, composition purity and crystal structure of the samples.
- By using this method transition of the phase from meso-phase to sub-state phase can be avoided.

2.5   Molecular beam epitaxy

This technique is used for the fabrication of nanoparticles in ultra-high vacuum. The rate of deposition which is typically 3000 nm per hour or less is one of the most important factor responsible for the crystalline overlayer growth of the films. The films grown on the surface of the crystalline substrate have better purity as there are no gases that can react in an ultra-high vacuum used in the reactions.

There are effusion cells in which the elements are heated in solid source molecular beam epitaxy. Reflection high energy electron diffraction is the equipment that is used to monitor the overlayer growth of the crystal. With a help of a powerful computer, the thickness of the layer or film can be controlled. Due to this fact, this technique is one of the most desirable for the fabrication of quantum dots as well as quantum wells. Nowadays, in semiconductor industry the control over the thickness of layers are very critical for devices like semiconductor lasers and LEDs. The ultra-high vacuum environment is created using cryopumps and liquid nitrogen is used to cool down the substrate in those reactions where it needs to be cooled. The maintenance of the cryogenic temperatures is used to trap impurities in the vacuum so the ultra-

high vacuum guarantees the deposition of high purity films. Molecular beam epitaxy can be used to fabricate organic semiconductors. This is made possible by making the molecules evaporate and the depositing it on to the substrate. There is another variation known as gas-source molecular beam epitaxy which is similar to the chemical vapour deposition. Molecular beam epitaxy can be modified as per needs such as inclusion of oxygen sources, which is helpful for the deposition of the oxide materials.

This process provides the precise control over composition and morphology of the prepared samples. A base material is used for the start of the process which is known as substrate. Typical semiconductors like silicon, germanium etc can also be used as a substrate. The process involves the heating of the substrate to some hundreds of degrees. After the heating process, the substrate is fired by a very precise beam of atoms that are produced by the effusion cells that are typically known as guns. One effusion cell is used to bombard a single beam on the sample you want to fabricate. The molecules fired from the guns hit the surface of substrate, they build up there slowly and condense resulting in the production of the single later of sample you want to create.
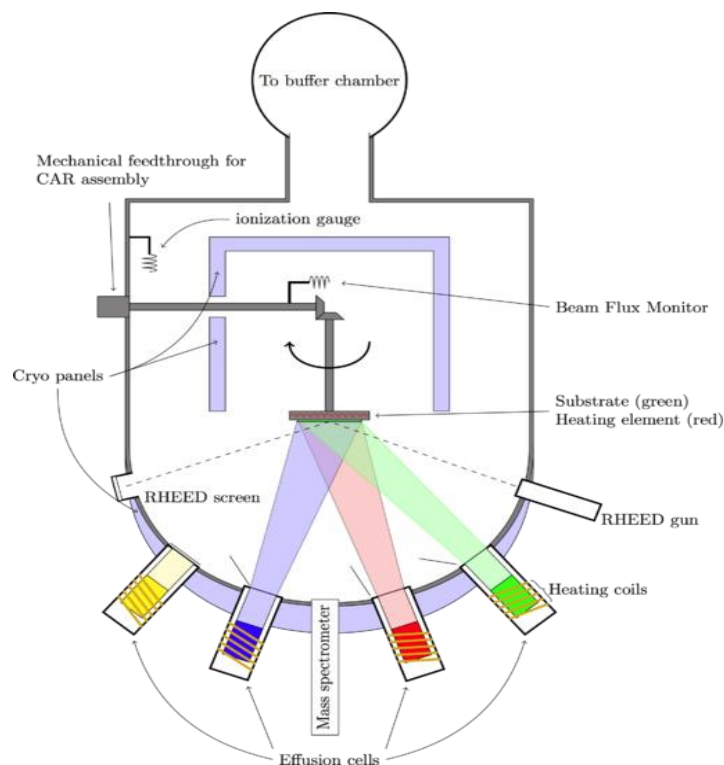
Fig 2.5: Molecular beam epitaxy [90].

CHAPTER 3: Characterization Techniques

This chapter includes the following techniques that can be used for material characterization in nano range.

- X ray diffraction (XRD)
- Scanning electron microscopy (SEM)
- LCR meter
- Super conducting quantum interference device (SQUID)
- Fourier transform infrared spectroscopy technique (FTIR)

3.1 X-Ray diffraction (XRD)

3.1.1 Introduction

This is the technique that uses X-Rays to characterize the material by determining and the size of the unit cells of the crystal structure because unit cell can be characterized as the main entity or the basic building block of crystal structures. The X-rays which are used in XRD techniques are actually electromagnetic waves which have the wavelength which is approximately equal to 1 Angstrom, which is equal to the size of atom.

The X-Rays are bombarded on the material under examination when the X-Ray strikes the surface of the material some of the rays enter the material and destructive interference as well as constructive interference occurs, and this is due to the atomic planes that have spaces between them. X-ray diffraction pattern is very useful in following areas that are very important.

- Determining the structure of crystalline material
- Characterization known as fingerprint

The patterns obtained by X-Ray diffraction are unique and can be identified using JSP cards etc. The determination of the structure of material is another field for which we use X-Ray crystallography. By using this technique, the interatomic spacing, bond angles as well as the packing fraction which tells, how the close the atoms are packed within the crystal structure can be determined.

3.1.2 Basic functionality

In XRD technique the production of X-Rays is very important process and the reason why X-rays are used is because these electromagnetic waves have the wavelength which is equal to the interatomic spacing within the crystal structure and it the angstroms. So, the structural information can only be determined by using electromagnetic waves in this frequency range and this requirement is fulfilled by X-Rays. There's a hot filament made up of tungsten and when this filament is heated the electrons come out of it and electrons striking the metal target give rise the production of X-Rays. When the incident electrons strike the other electrons that are present in the K-Shell of the metal they get ionized and because of this X-Rays are emitted from the target made up of metal and after that the vacancies, that were created by the incident electrons, are filled by the electrons which come from M and L shells of the target. When the X-Rays are incident on the surface of crystalline material, scattering occurs because of the distance between the atomic planes but one thing here to be noted is that the wavelength doesn't change. So, the scattering of X-rays occurs in some directions where constructive interference takes place. Because some of the X-Rays are in phase at that point and time but there are a lot of X-Rays that are not in phase which result in the phenomenon of destructive interference and this is actually known as diffraction.

These diffracted X-Rays are the source of the information that reveals the dimensions of unit cells and is useful for the analysis and characterization of crystalline material. The arrangement of the atoms in the crystalline materials is very crucial for characterizing any crystalline material and the information about this arrangement is given by the diffracted X-Rays that are in phase (Constructive interference). If the distance between the atoms of the material is not of the order of the wavelength of incident X-Rays then no information about the crystal structure can be obtained.

3.1.3 The Bragg Law

The equation for the diffraction was given by W.L. Bragg, In early 20th century. This equation made it possible for us to mathematically calculate the diffraction from the planes off the unit cells.

$$n\,\lambda = 2d\,\sin(\theta)$$
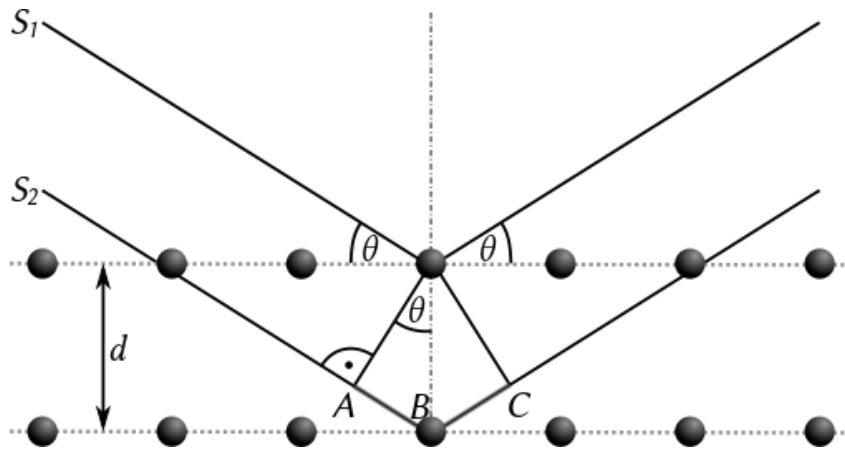
Fig 3.1.3: Phenomenon of diffraction [91].

The fulfilment of the following condition will result in constructive interference only.

$n\lambda = AB + BC$

We can see in the figure $AB = BC$

This states, $n\lambda = 2AB$

$\text{Sin}(\theta) = AB/d$ (figure 3.1.3)

$AB = d \, \text{Sin}(\theta)$

$n\lambda = 2d \, \text{Sin}(\theta)$

The inter atomic spacing of the crystal structure is denoted by 'd', θ refers to incident angle where 'n' is an integer and 'λ' is the wavelength of the incident X-Rays which are of the order of Angstrom or equal to the dimensions of atoms.

3.2 Scanning Electron Microscopy (SEM)

Scanning electron microscope is an instrument used in scanning electron microscopy for the compositional characterizations of the samples, and this highly adaptive instrument is being used for the examination and analysis of the micro structures. With the help of optical microscopes, the objects, that are smaller than 2000 angstroms, cannot be discriminated and human eye can only see the objects greater than 0.1 mm in dimension before 1890's optical microscopy was of great importance and scientific research before the discovery of the microscopes that use electron beam for the characterization of materials that are of the order of nanoscale (few nano-meters). After the discovery of the fact that it is possible to deflect electrons by using magnetic fields electron microscopy took the place of optical microscopy. As the electron beam with high energy is used in SEM so the images with very high resolution can be obtained.

3.2.1 The Abbe Equation and Resolution

Following equation that was given by the renowned scientist Ernst Abbe can be used to describe the resolution of perfect or ideal optical systems.

$d = 0.612 \, (\lambda) \, / \, n \, \text{Sin} \, (\alpha)$

In this equation we have

- The resolution is represented by "d"
- For the representation of wavelength "λ" is used.
- "α" represents the half angle in radiance of aperture.
- The refractive index of medium is denoted by "n".
- n Sin α is the representation of numerical aperture.

We're going to have to understand the limit of resolution. If there're two objects placed very closed to each other at minimum distance then by using some equipment we are able to see both the objects distinctively. This phenomenon is known as limit of resolution.
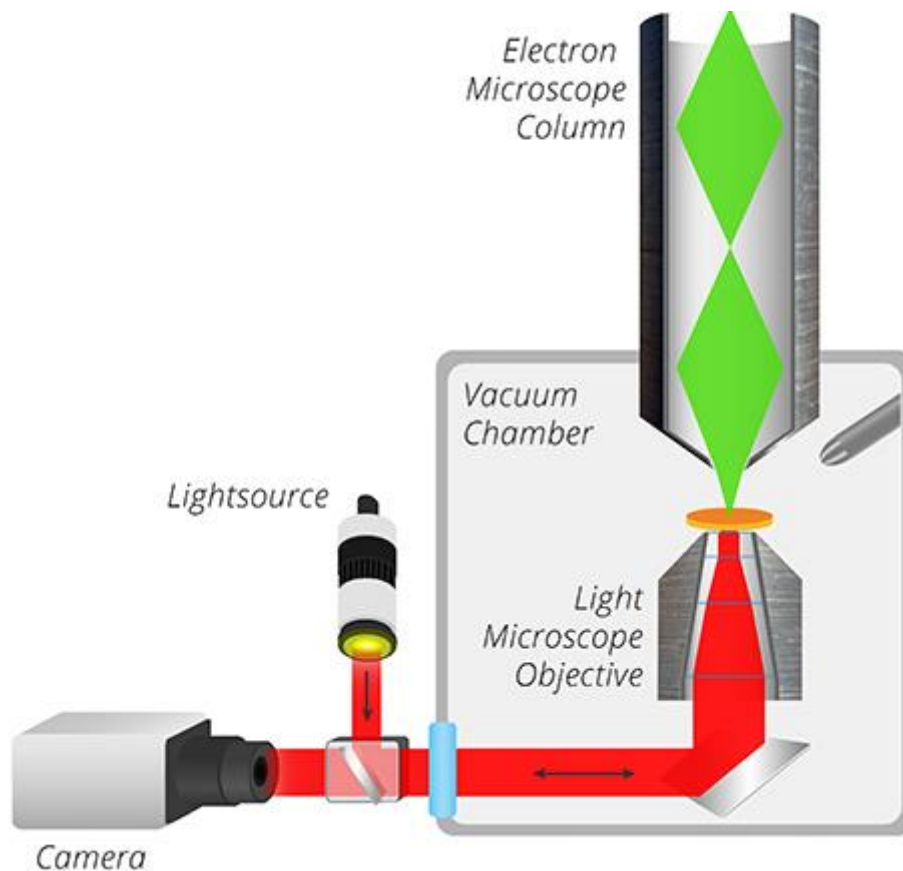

Fig 3.2.2: Schematic of SEM [92].

3.2.2 Interaction of electrons with sample

High resolution images obtained by SEM are the result of the signals that are generated when the electron beam interacts with the target being analyzed. There are two types of interactions which can be characterized as

1. Elastic interaction with sample
2. Inelastic interaction with sample

The deflection of electrons by the nucleus of the sample or if the electrons are deflected by the electrons of similar energy which is present in the outer shell of the specimen. This type of deflection or scattering is known as elastic scattering. Very small amount of energy is dissipated in this kind of wide angles scattering. If the angle of scattering is more than 90 degrees than back scattered electrons are emitted and these electrons are very important for the formation of image of the sample as they provide very useful signals in this regard. The electrons that are scattered by the atoms and electrons that are present in the sample give rise to inelastic scattering. The loss of energy is determined by the binding energy of the excited electrons in an inelastic scattering. The production of the secondary electrons is the result of this type of scattering as they have the energy less than 50eV and these secondary electrons are very important and useful for the formation of high resolution SEM images. There is a wide variety of signals that are generated by the virtue of interacting electron beam and the constituents of specimen and these include Auger electrons and X-Rays etc. There are some high energy electrons that spike in to the sample instead of reflecting back and they give rise to the number of different signals because they create a region in the sample known as primary region.

3.2.3 Secondary electrons

This type of electrons are the result of the emission of the electrons from the sample's surface when the interaction of electrons and surface of sample occur. The signals that are generated by these secondary electrons that are generated due to the interaction of primary beam with electrons of the sample is most important for the formation of images and SEM. The topographic analysis of the sample is very useful to analyse the surface of the sample is made possible by these secondary electrons. The secondary electrons penetrate few nano-meters inside the surface of the sample and precise position of the electron beam can be marked as they possess very low energy they can move toward the detector as well. The images that are obtained by these secondary electrons have the resolution of 10 nano meters. The

information about the texture and roughness (topographic information) can be obtained by these secondary electrons. This topographic information is obtained when these secondary electrons reach the detector and the ones that do not reach the detector are responsible for shadows that can be seen in the SEM image.

3.2.4   Back scattered electrons

These electrons are helpful in giving the information about the roughness and the texture of the surface. In order to form image in SEM there's a technique developed that helps to detect technique by which these back scattered electrons are detected. These electrons possess energy which is greater than 50eV and these are scattered more than one time.

As the back scattered electrons have very high energy so when they collide elasticity with the nucleus of the target atom. These electrons bounce back towards their source and nearly half of the electron beam back scatters. The high energy of the electrons is the cause of the bouncing back of these electrons instead of absorbing in the sample, So the producing area of back scattered electrons become larger than the region of production of the secondary electrons and this large area results in the poor resolution as compared to the resolution of images formed by secondary electrons.

Secondary electrons give the information about the surface of the sample and the information below the surface of the sample as well as topographic information is given by the back scattered electrons. And this is the major difference between both of these electrons. There's a difference between the images produced by these back scattered electrons and secondary electrons because some regions are generated which prevent the generation of back scattered electrons.

3.3   LCR meter

The device used for measuring inductance, capacitance and resistance of the material under observation is known as LCR. As the name suggests, L denotes inductance, Capacitance is denoted by C and R is for the representation of resistance. The capacitance is the measure of the capability of the capacitor to store charge. Resistance is the term used to refer the opposition by the material to the charges. The measurement of the "dissipation factor" as well as "quality factor" can be made using LCR meter. Other useful parameters like, current, voltage, the phase angle made by the current and voltage, conductance and susceptibility.

3.3.1 Working Principle

The calculation of the current and the voltage through the device under examination and an alternating current is flowing through the device. LCR meter is not designed to measure inductance, resistance and capacitance directly but if the impedance of the device is known then these various components can be determined. Impedance is a measure of the opposition to alternating and direct current. The dependence of this vector quantity is on two scaler quantities, that are resistance and reactance. The complete opposition because of the inductance and capacitance is termed as reactance.

3.3.2 Techniques used in LCR meter

Following are the two techniques that are used in LCR meter for the determination of various parameters.

1. Current-voltage measurement technique.
2. Bridge technique.

- **Current-voltage measurement technique**

In this technique determining the values of current and voltage enable to find values of impedance of the device under test. Whereas the arrangement of the circuit is crucial for finding the values of low and high impedance. Both uses different configurations of circuits that are shown in the figure. This method is suitable for the applications at high frequency range.
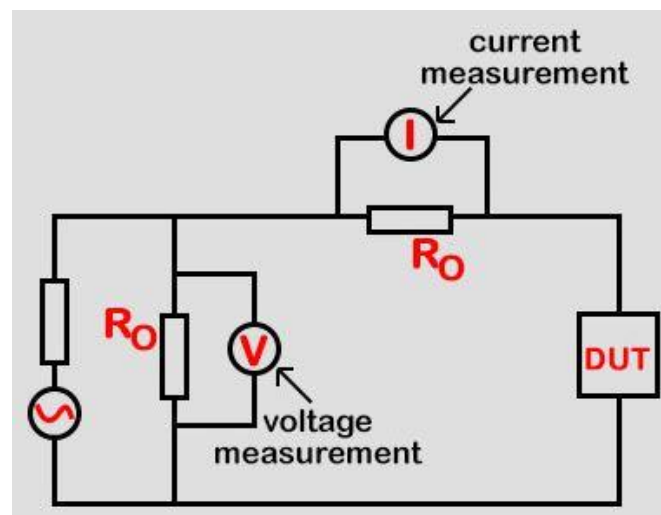
Fig 3.3.2 (a): Circuit diagram of LCR meter for high impedance [93].
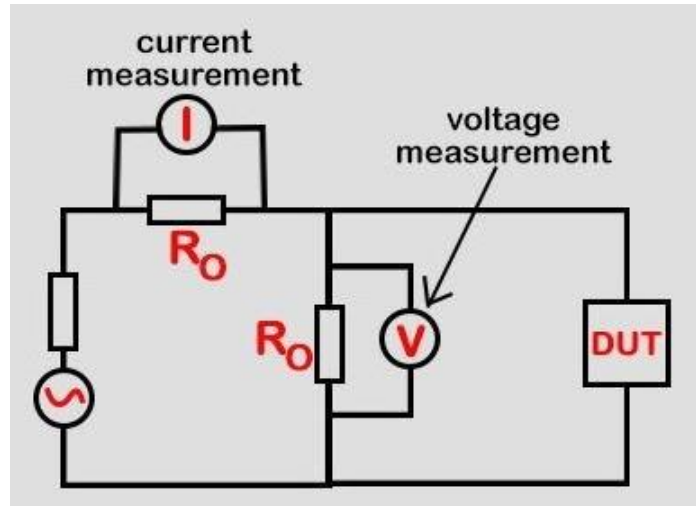
Fig 3.3.2(b): Circuit diagram of LCR meter for low impedance [93].

- **Bridge technique**

    To check whether the device or material under test have some low range frequency applications, this technique is the most suitable. In this method, the measurement of the samples is carried out under the frequency of 100 kilohertz. The principle used in this technique is known as Wheatstone bridge principle. Wheatstone bridge circuit is shown in the figure. In the figure the impedances Z2 and Z4 have the values that are known and the material under test with its impedance Zu is put at the position as shown in the figure. This configuration depicts the bridge like structure. Now what happens is the flow of current through the device under test changes the impedance that is denoted by Z1, then the following expression gives the value of an unknown impedance at the balance position.

Z1/Zu=Z3/Z4

Fig 3.3.2(c): Bridge technique for LCR meter [94].

3.4   Super conducting quantum interference device (SQUID)

A Super conducting quantum interference device is used for the measurement of very weak magnetic fields. This device is extremely sensitive and has the capability to measure very weak magnetic fields of the order of about 5 aT. We see the wide spread of this device in different biological studies, r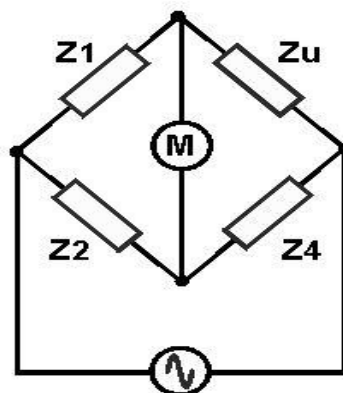esearch, and for the measurement of ultra-sensitive electronic and magnetic systems where the conventional instruments fail to sense any information what so ever.

3.4.1   Explanation

SQUID consists of a superconducting loop that contains one or more junctions named as Josephson junction.

There are two types of SQUIDs available in the market.

1. Radio frequency (RF) SQUID.
2. Direct current (DC) SQUID.

The radio frequency SQUID has a single Josephson junction, while the DC SQUID has two or more Josephson junctions. The Radio frequency SQUID is relatively less sensitive as compared to the Direct current SQUID.

Normally, Direct current SQUID consists of a superconducting loop in which two parallel junctions are inserted. The input current is divided equally to the two junctions when the magnetic field is not present. When the external magnetic field is provided, the resonant frequency changes and this change triggers a change in voltage between the junctions. This change in voltage can be used to calculate the values of magnetic flux as the voltage is a function of magnetic flux.

Niobium and pure lead alloys are superconducting material that are used in SQUIDs to work in low temperatures. Helium is used for cooling the device as it has to be very cool in order to maintain superconductivity. But for the high-temperature super conducting quantum interference device to work, yttrium barium copper oxides that is a high-temperature superconductor and this device is cooled by using liquid nitrogen as a cooling agent. The low-temperature SQUIDs are more efficient than the high-temperature SQUIDs.

3.4.2   USES of SQUIDs

- It is used for detecting magnetic energy fields that are so weak that their magnitude is about 100 billion times smaller as compared to the magnetic energy required to move a magnetic compass needle.

- SQUIDs are used for the measurement of weak signals from the human mind and human heart.

- SQUID is used to construct very sensitive gradiometers.

- This device is used in magnetometers and voltmeters.

3.5   Fourier transform infrared spectroscopy (FTIR)

FTIR technique was developed in early 1970s. FTIR is a characterization technique used for obtaining emission or absorption spectrum of solids, liquids and gases within infrared range. It consists of a spectrometer that is used for the collection of spectral data over a wide infrared range. The data given by the spectrum is converted using the fourier transform, which is a name of a mathematical process.

3.5.1   Basic components of FTIR

Components of the Fourier transform Infrared spectroscopy is shown in the figure. In this technique, the infrared radiations containing various wavelengths are emitted by an infrared source. The modulation of the infrared radiations occurs in the interferometer when the radiations pass through it. Optical inverse Fourier transform is performed on the incident radiations. Then the beam pass through the sample where molecules in the samples are responsible for the absorption of incident radiation at various wavelengths. Finally, the detector detects the intensity of the IR radiations. The IR spectrum is obtained after the fourier transform is applied by the computer on the detected signal after the analog signal is converted into digital signal.
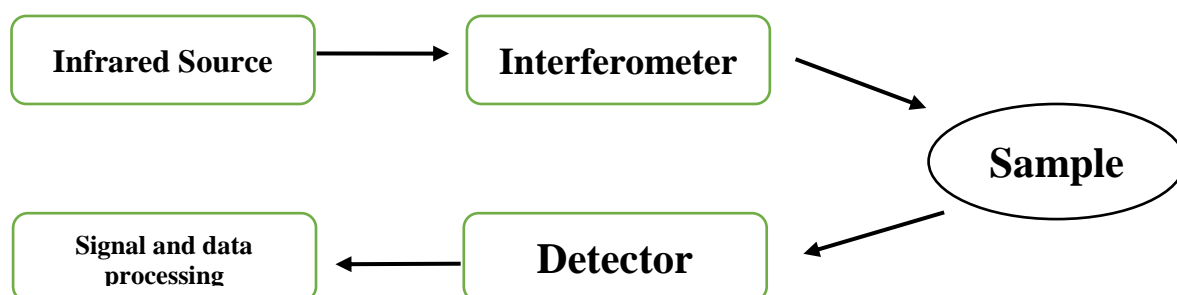

Fig 3.5.1(a): Schematic of FTIR

One of the component of an FTIR spectrometer is the interferometer. The interferometer is shown in the figure which resembles the Michelson interferometer. One half of the incident radiation is transmitted through the beam splitter and the other half is reflected. This phenomenon is same as the working of Michelson interferometer.
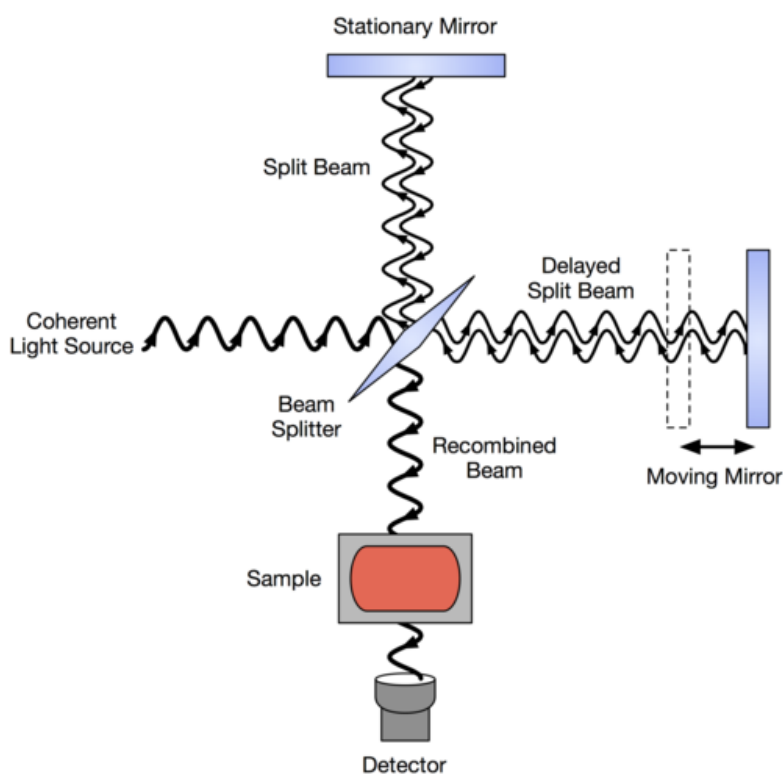
Fig 3.5.1(b): Working of FTIR [95].

When the interference occurs, the detected signal is measured by the detector which depends on the difference of optical path length, this measured signal is called interferogram. The intensity is shown as the function of displacement produced by the moving mirror in a typical interferogram. At different wavelengths, the number of radiations absorbed by the material is quantitatively related to the number of molecules that are responsible for the absorption of radiations in the sample. The relationship between the degree of absorption by the sample and the number of absorbing molecules is linear, which ensures the multicomponent quantitative analysis.

3.6 Experimental Procedure

The fabrication $Bi_{1-x}Gd_xFe_{1-y}Sn_yO_3$ (BGFSO, x=0, 0.1, 0.15, 0.25; y= 0, 0.1) abbreviated as BiFeO3 (BFO), $Bi_{1.0}Gd_{0.0}Fe_{0.90}Sn_{0.10}O_3$ (BGFSO-0Gd), $Bi_{0.9}Gd_{0.1}Fe_{0.90}Sn_{0.10}O_3$

(BGFSO-10Gd), $Bi_{0.85}Gd_{0.15}Fe_{0.90}Sn_{0.10}O_3$ (BGFSO-15Gd), $Bi_{0.75}Gd_{0.25}Fe_{0.90}Sn_{0.10}O_3$ (BGFSO-25Gd) nanoparticles was carried out using double solvent sol-gel method. The $Bi(NO_3)_3 \cdot 5H_2O$ (Bismuth nitrate pentahydrate) (99% pure) and $Gd(NO_3)_3 \cdot 6H_2O$ (Gadolinium nitrate) (99.9% pure) were mixed while maintaining stoichiometry, then the mixture was dissolved in acetic acid $[C_2H_4O_2]$ and ethylene glycol $[C_2H_6O_2]$, and the solution was stirred for 90 minutes at room temperature (RT). Tin (Sn) powders and $Fe(NO3)_3 \cdot 9H_2O$ (Iron nitrate nanohydrate) (98.5% pure) were dissolved in acetic acid $(C_2H_4O_2)$ and magnetic stirring was carried out constantly for 1 hour and 30 minutes. After stirring for 1.5 h, both the solutions were mixed together and again set to constant stirring for 3 hours.

A uniform and very fine precursor solution of molarity 0.4 M which was reddish brown in colour was produced. The solutions were fabricated with 3 percent more Bi because the loss of bismuth during the heating process has to be compensated. The solvent used in the process was ethylene glycol which ensured the electronegativities of Fe and Bi during the reaction. During the fabrication process the chemical reaction was controlled by acetic acid which was used as a catalyst, it also maintained the concentration of the solution. The drying of the prepared solution in an oven at 80 ºC resulted in a gel after 12 hours. After that calcination was done in furnace at 600 ºC for 3 hours. Finally, a fine powder was obtained after crushing.

Chapter 4: Results and Discussion

4.1 Crystal structure and Phase analysis

The phase and the crystal structure of the prepared samples $Bi_{1-x}Gd_xFe_{1-y}Sn_yO_3$ (BGFSO, x=0, 0.1, 0.15, 0.25; y= 0, 0.1) were investigated by XRD analysis and the resulted data is shown in the fig. The pattern shown by Pure BFO is in accordance with the rhombohedral structure of the bismuth ferrite $BiFe_2O_3$ system (JCPDS card no. 20-0169) having R3c space group. The shift in peaks and the peak merge of the doped BFO can be attributed to the substitution of the Gd and Sn impurities in different proportions.
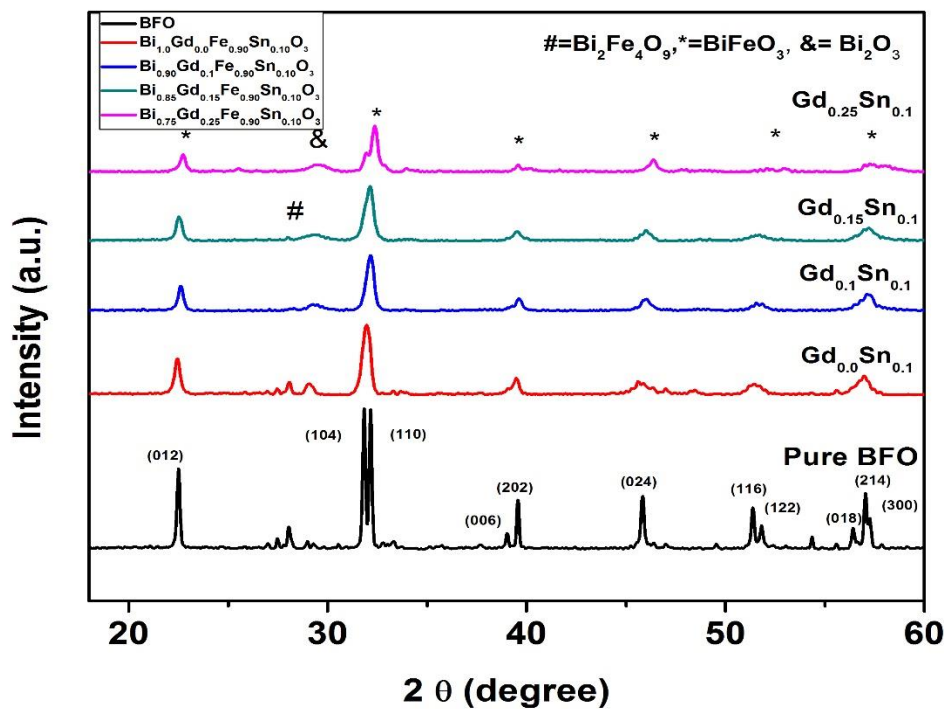
Fig 4.1: XRD of $Bi_{1-x}Gd_xFe_{1-y}Sn_yO_3$ (BGFSO, x=0, 0.1, 0.15, 0.25; y= 0, 0.1)

Moreover, samples with higher concentration of Gd showed broader peaks. The disappearance of the doublet peaks of the pure BFO, by increasing the Gd substitution, can be the result of phase transition from the rhombohedral to orthorhombic [97]. There are some other reports also support this phenomenon [98,99].

The revelation of the two peaks, as indicated in the XRD patterns of $Bi_{0.85}Gd_{0.15}Fe_{0.90}Sn_{0.10}O_3$ and $Bi_{0.75}Gd_{0.25}Fe_{0.90}Sn_{0.10}O_3$ is due to the presence of the impurity phase of $Bi_2Fe_4O_9$ and

Bi$_2$O$_3$. Also, the peak corresponding Bi$_2$Fe$_4$O$_9$ vanishes when Gd concentration is increased. This non-perovskite Bi$_2$Fe$_4$O$_9$ secondary phase was also observed in pure BFO and Gd doped BFO (Bi$_{0.95}$Gd$_{0.05}$FeO$_3$) in other report [100].

4.2 Structural Analysis and Morphology

There are clear voids or pores that can be seen in the images of samples generated by SEM and the reason can be well linked to the liberation of different gases during the combustion process. The characteristics of the combustion synthesized powder are also depicted in the form of porous network of particles and the presence of clusters of agglomerated particles. The introduction of the different concentrations of Gd resulted in the particle size reduction. The phase transition from rhombohedral to orthorhombic and the agglomeration of particles can be attributed to the addition of Gd substitutions to the BFO [101]. The variation in size of the particles can also be explained in the light of Kirkendall effect that, in the doping process, arises due to the different diffusion rates of the constituting elements [102].
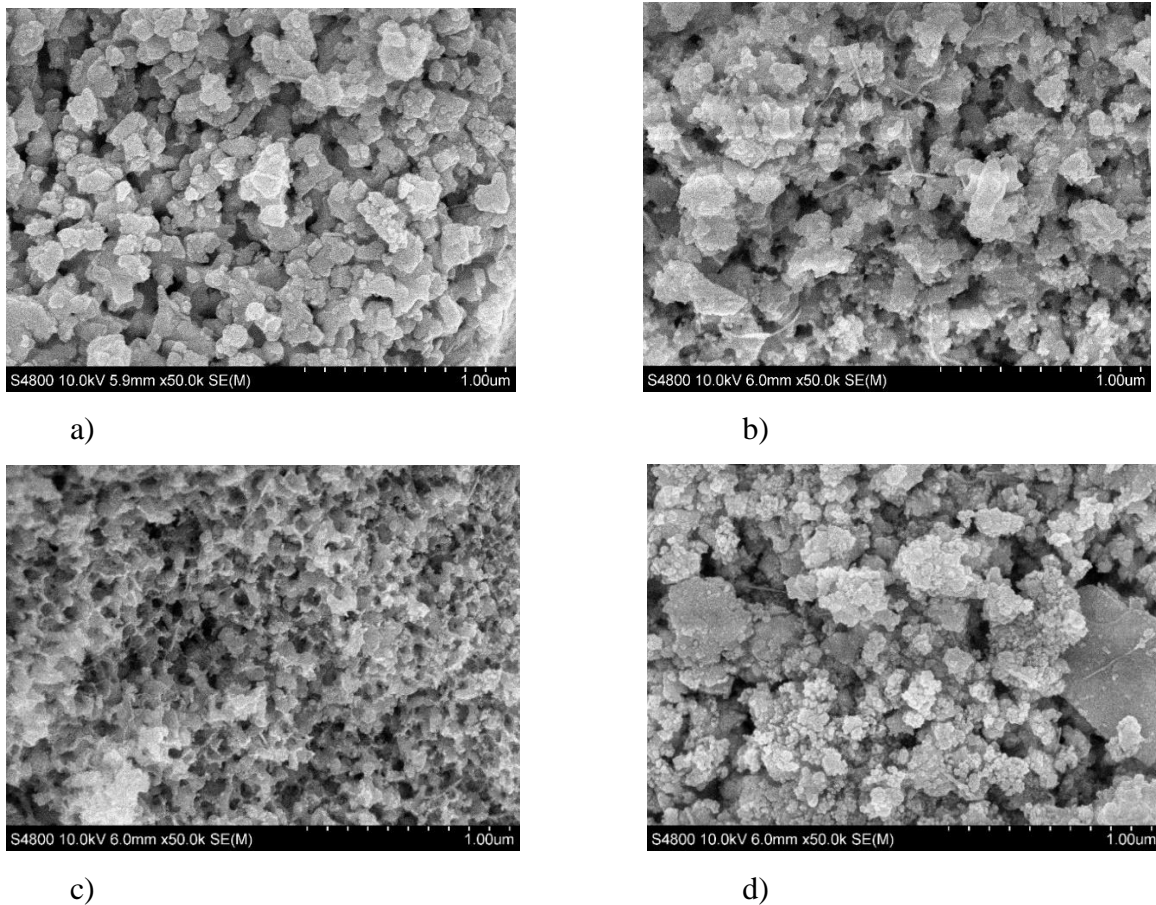

a)

b)

c)

d)

Fig 4.2: a) BGFSO (Gd 0%), b) BGFSO (Gd 10%), c) BGFSO (Gd 15%), d) BGFSO (Gd 25%)

4.3   Dielectric Constant and Dielectric Loss:

Dielectric loss and the Dielectric constant as a function of natural logarithm of frequency are shown in the figure. From figure, Similar behavior can be seen for all the samples, show significant change due to the variations in frequency. The values of dielectric constant and dielectric loss were significantly decreased with the increase in frequency but showed no dependence on frequency at the higher frequencies. This behavior can be attributed to dielectric relaxation phenomenon in which the dipoles that are created inside the material changes polarity according to the frequency of the applied field at low frequency range [103, 104]. But at the higher frequencies the time required by the atoms present in the dielectric material to change their direction becomes very large as compare to the rate of the polarity change of applied filed and thus no higher frequency dependence of dielectric loss can be observed. This argument is also supported by the Koop's theory.

The maximum dielectric loss of the pure BFO sample arises due to the generation of oxygen ion vacancies by oxygen loss and Fe^{3+} ions that reduce to Fe^{2+} [105]. These oxygen ions vacancies suppressed by the co-doping of Gd and Sn and this improves the dielectric loss factor as shown in the figure.

From figure, AC conductivity of the samples increases with the increase in frequency because at the higher frequencies the value of dielectric loss tends to decrease due to the very large rate of polarization of the applied field and so decrease in loss enhanced the conductivity of the samples.
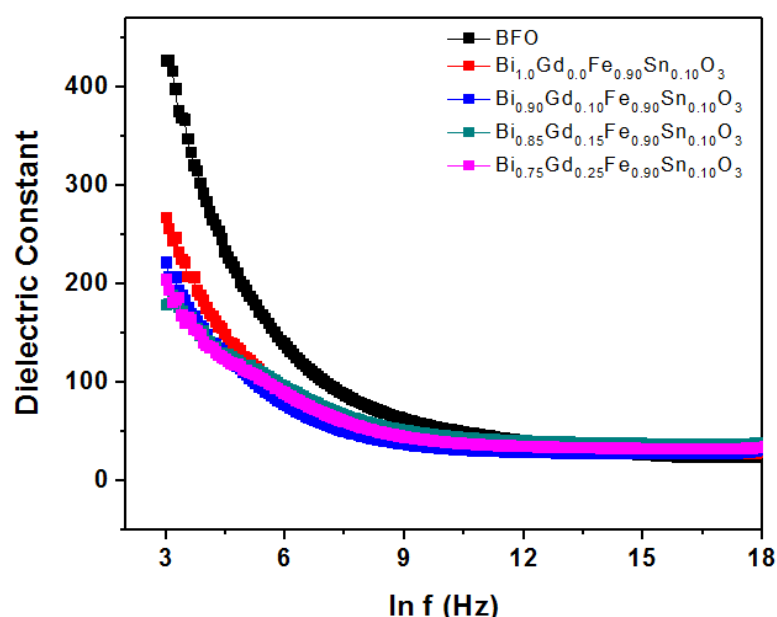

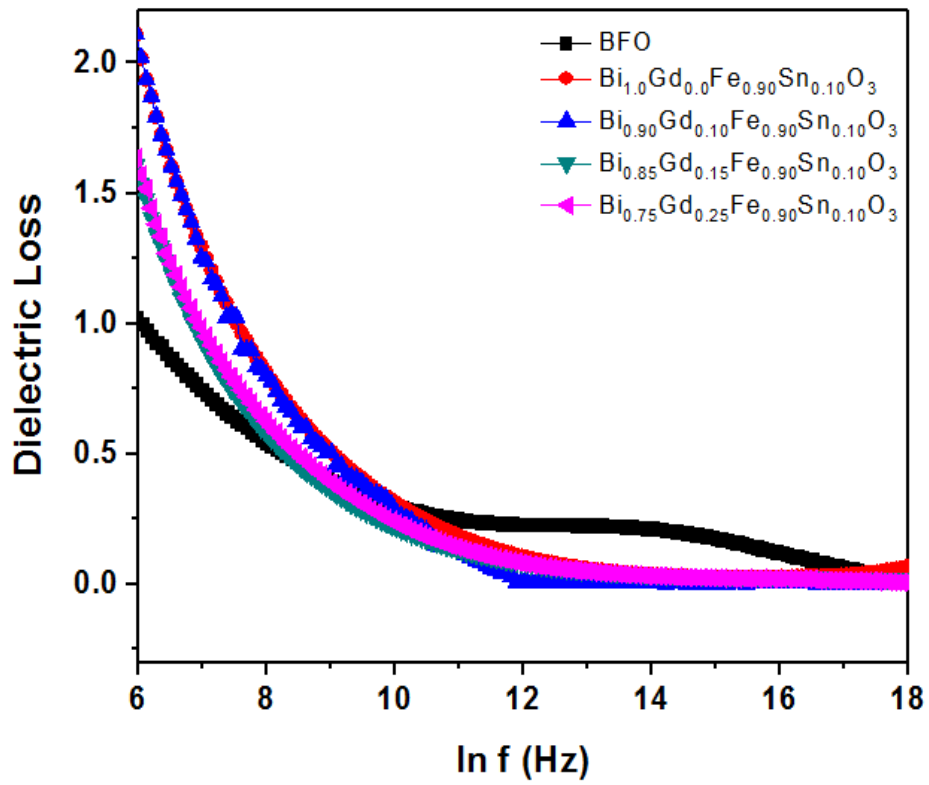**Fig 4.3(a)**: Dielectric constant of Gd and Sn co-doped BFO.

Fig 4.3(b): Dielectric Loss of Gd and Sn co-doped BFO.
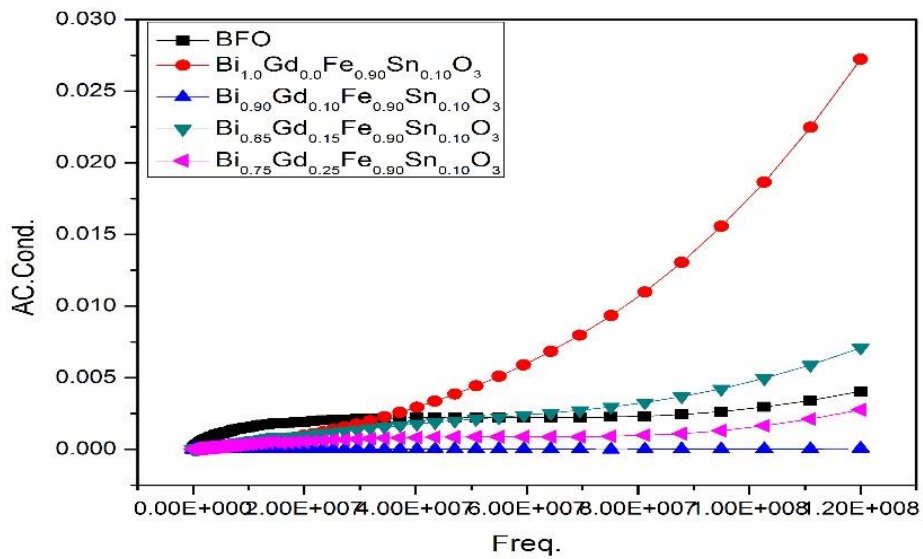
Fig 4.3(c): AC Conductivity of Gd and Sn co-doped BFO.

4.4   Magnetic Properties:

Figure reveals a clear hysteresis behavior for all the samples of doped BFO except the bulk BFO which exhibits antiferromagnetic behavior at room temperature because of its G-type antiferromagnetic ordering. The increase in Gd substitutions in the BFO host increase the magnetic behavior of BGFSO samples. The saturation magnetization increases with the increase in the concentration of Gd (a rare-earth metal) in the samples.
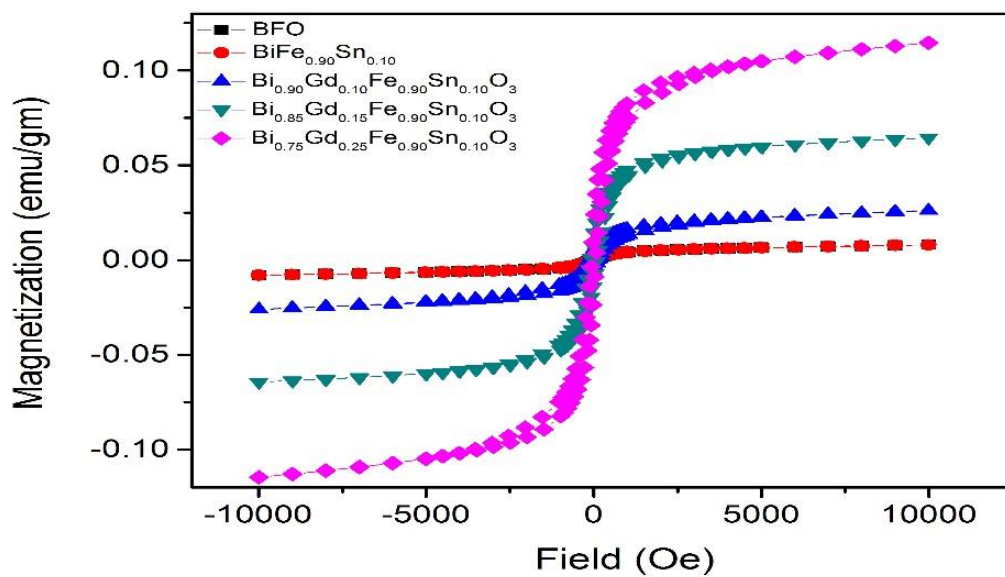
Fig 4.4: M-H Curves of Gd and Sn co-doped BFO

There can be multiple factors that can contribute to such enhancements in saturation magnetization. First, with the decrease in particle size, the very large surface to volume ratio alters the antiferromagnetic ordering at the surface of the particle and the net magnetization increases due to uncompensated ferromagnetic spins [106]. Second, the substitution of Gd ions in BFO lattice leads to the phase transition from the rhombohedral to orthorhombic structure that results in the enhancement of net magnetization with the increment of Gd content in BFO samples. The distortion in the rhombohedral perovskite structure generate a weak ferromagnetic ordering which results from the canting of spins [107-109]. Third, like other rare earth ion substitution, Gd ions at Bi-site can cause a space modulated spin to collapse and produce long-range antiferromagnetic order that enhances the value of net magnetization. Also, characteristic of Gd like distorted spin cycloid can also be the cause of increase in saturation

magnetization of the BFO samples. Fourth, the increase in number of Fe ions and decrease in oxygen vacancies due to co-doping can significantly enhance the values of saturation magnetization for different samples [110]. Fifth, the reduction in the size of small particles to around or below 62nm can break the periodicity of the spin cycloid which also results in the enhancement of saturation magnetization [111].

4.5   Fourier Transform Infrared Spectroscopy (FTIR)

FTIR Spectra of the $Bi_{1-x}Gd_xFe_{1-y}Sn_yO_3$ (BGFSO, x=0, 0.1, 0.15, 0.25; y= 0, 0.1) is shown in the figure. The revelation of different peaks around 560 in different samples is attributed to Fe-O stretching which is a characteristic of octahedral FeO_6 group in the compounds that have perovskite structure [112,113]. The existence of metal band at 500-600 confirms the formation of perovskite structure in prepared samples [114].

The peaks around 1387 cm^{-1} and 845 cm^{-1} indicates the presence of nitrate ions [115-117]. There is another peak at around 2333 that serve as the representative of a nitrile [118].
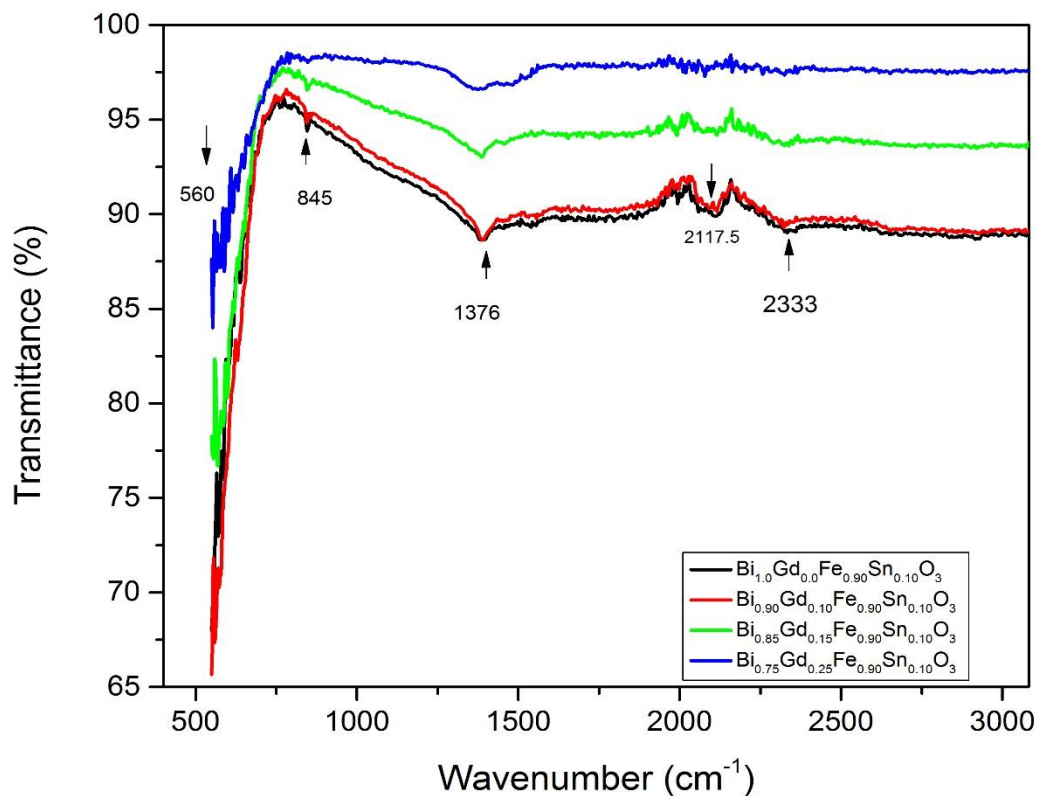
Fig 4.5: FTIR of Gd and Sn Co-doped BFO

4.6 Conclusion:

BFO nanoparticles were successfully prepared by double solvent sol-gel method. XRD patterns showed distorted rhombohedral structure of pure BFO which undergoes phase transition from rhombohedral to orthorhombic structure due to the Gd substitution in BFO. The Gd doping caused the average particle size to reduce also voids, porous networks and agglomeration was observed. Dielectric relaxation phenomenon was observed with no effect on dielectric behavior at higher frequencies. The hysteresis behavior was observed for different concentrations of magnetically active Gd added in BFO host, the increas in the values of saturation magnetization was observed with increase in the concentration of Gd, because of the change in antiferromagnetic ordering at the particle's surface, phase transition from rhombohedral to orthorhombic, collapse of space modulated spin, decrease in oxygen vacancies and increments in number of Fe ions.

REFERENCES

[1] Martin, Charles R. "Welcome to nanomedicine." *Nanomedicine* 1.1 (2006): 5-5.

[2] Zurek, Wojciech Hubert. "Decoherence, einselection, and the quantum origins of the classical." *Reviews of modern physics* 75.3 (2003): 715.

[3] Royal Society (Great Britain). *Nanoscience and Nanotechnologies: Opportunities and Uncertainties: Summary and Recomendations*. Royal Society, 2004.

[4] Speshock, Janice L., et al. "Interaction of silver nanoparticles with Tacaribe virus." *Journal of nanobiotechnology* 8.1 (2010): 19.

[5] Arivalagan, K., et al. "Nanomaterials and its potential applications." *Int. J. ChemTech Res* 3.2 (2011): 534-538.

[6] "File: Nanostructure geometries.jpg." *Wikimedia Commons, the free media repository*. 27 Nov 2014, 00:05

[7] Özgür, Ümit, Yahya Alivov, and Hadis Morkoç. "Microwave ferrites, part 1: fundamental properties." *Journal of Materials Science: Materials in Electronics* 20.9 (2009): 789-834.

[8] Harris, Vincent G. "Modern microwave ferrites." *IEEE Transactions on Magnetics* 48.3 (2012): 1075-1104.

[9] Nathani, H., and R. D. K. Misra. "Surface effects on the magnetic behavior of nanocrystalline nickel ferrites and nickel ferrite-polymer nanocomposites." *Materials Science and Engineering: B* 113.3 (2004): 228-235.

[10] Pullar, Robert C. "Hexagonal ferrites: a review of the synthesis, properties and applications of hexaferrite ceramics." *Progress in Materials Science* 57.7 (2012): 1191-1334.

[11] Pullar, R. C., and A. K. Bhattacharya. "Crystallisation of hexagonal M ferrites from a stoichiometric sol–gel precursor, without formation of the α-BaFe 2 O 4 intermediate phase." *Materials Letters* 57.3 (2002): 537-542.

[12] "File: Crystal structure of Ferrite spinel.png." *Wikimedia Commons, the free media repository*. 25 Nov 2016, 15:53

[13] Šepelák, V., et al. "The mechanically induced structural disorder in barium hexaferrite, BaFe 12 O 19, and its impact on magnetism." *Faraday discussions* 170 (2014): 121-135.

[14] Wang, J., et al. "M., Wuttig, and R. Ramesh." *Science* 299 (2003): 1719.

[15] Lebeugle, Delphine, et al. "Room-temperature coexistence of large electric polarization and magnetic order in Bi Fe O 3 single crystals." *Physical Review B* 76.2 (2007): 024116.

[16] Wen, Zheng, et al. "Effects of annealing process and Mn substitution on structure and ferroelectric properties of BiFeO 3 films." *Thin Solid Films* 517.16 (2009): 4497-4501.

[17] Gupta, Surbhi, et al. "Piezoresponse force microscopy and vibrating sample magnetometer study of single phased Mn induced multiferroic BiFeO3 thin film." *Journal of Applied Physics* 111.6 (2012): 064110.

[18] Scott *et al.*,"Multiferroic and magnetoelectric materials" Nature Reviews,**442**, (2009) 759.

[19] Park, Tae-Jin, et al. "Size-dependent magnetic properties of single-crystalline multiferroic BiFeO3 nanoparticles." *Nano letters* 7.3 (2007): 766-772.

[20] Seshadri, Ram, and Nicola A. Hill. "Visualizing the role of Bi 6s "lone pairs" in the off-center distortion in ferromagnetic BiMnO3." *Chemistry of materials* 13.9 (2001): 2892-2899.

[21] "File: Multiferroics history use of terms magnetoelectric and multiferroic.png." *Wikimedia Commons, the free media repository*. 14 Jan 2015, 03:01

[22] Kiselev, S. V., R. P. Ozerov, and G. S. Zhdanov. "Detection of magnetic order in ferroelectric BiFeO3 by neutron diffraction." *Soviet Physics Doklady*. Vol. 7. 1963.

[23] Zhao, T., et al. "Electrical control of antiferromagnetic domains in multiferroic BiFeO3 films at room temperature." *Nature materials* 5.10 (2006): 823-829.

[24] Teague, James R., Robert Gerson, and William Joseph James. "Dielectric hysteresis in single crystal BiFeO3." *Solid State Communications* 8.13 (1970): 1073-1074.

[25] Sosnowska, I., T. Peterlin Neumaier, and E. Steichele. "Spiral magnetic ordering in bismuth ferrite." *Journal of Physics C: Solid State Physics* 15.23 (1982): 4835.

[26] Michel, Christian, et al. "The atomic structure of BiFeO3." *Solid State Communications* 7.9 (1969): 701-704.

[27] Kubel, Frank, and Hans Schmid. "Structure of a ferroelectric and ferroelastic monodomain crystal of the perovskite BiFeO3." *Acta Crystallographica Section B: Structural Science* 46.6 (1990): 698-702.

[28] Silva, J., et al. "BiFeO3: a review on synthesis, doping and crystal structure." *Integrated Ferroelectrics* 126.1 (2011): 47-59.

[29] Sharma, H. B., et al. "Structural and optical properties of manganese substituted nanocrystalline bismuth ferrite thin films by sol–gel process." *Journal of Alloys and Compounds* 583 (2014): 106-110.

[30] Li, Yongtao, et al. "Magnetic properties and local structure of the binary elements codoped Bi 1− xLaxFe 0. 95 Mn 0. 05 O 3." *Journal of Alloys and Compounds* 592 (2014): 19-23.

[31] Wu, Chunfang, Jie Wei, and Fansheng Kong. "Effect of rare earth dopants on the morphologies and photocatalytic activities of BiFeO3 microcrystallites." *Journal of Materials Science: Materials in Electronics* 24.5 (2013): 1530-1535.

[32] Fei, Linfeng, et al. "Electrospun bismuth ferrite nanofibers for potential applications in ferroelectric photovoltaic devices." *ACS applied materials & interfaces* 7.6 (2015): 3665-3670.

[33] Pei, Yan-Ling, and Chaolei Zhang. "Effect of ion doping in different sites on the morphology and photocatalytic activity of BiFeO 3 microcrystals." *Journal of Alloys and Compounds* 570 (2013): 57-60.

[34] Basu, S., et al. "Enhanced magnetic properties in hydrothermally synthesized Mn-doped BiFeO 3 nanoparticles." *Current Applied Physics* 11.4 (2011): 976-980.

[35] Zheng, X. H., et al. "Synthesis and dielectric properties of BiFeO3 derived from molten salt method." *Journal of Materials Science: Materials in Electronics* 23.5 (2012): 990-994.

[36] Guo, Renqing, et al. "Enhanced photocatalytic activity and ferromagnetism in Gd doped BiFeO3 nanoparticles." *The Journal of Physical Chemistry C* 114.49 (2010): 21390-21396.

[37] T.T. Carvalho, J.R.A. Fernandes, J. Perez de la Cruz, J.V. Vidal, N.A. Sobolev, F. Figueiras, S. Das, V.S. Amaral, A. Almeida, J. Agostinho Moreira, P.B. Tavares, J. Phys. Chem. C 511 (2012) 149–153.

[38] X.W. Tang, J.M. Dai, X.B. Zhu, Y.P. Sun, J. Phys. Chem. C 511 (2012) 149–153.

[39] Kothari, Deepti, et al. "Study of the effect of Mn doping on the BiFeO3 system." *Journal of Physics: Condensed Matter* 19.13 (2007): 136202.

[40] Coondoo, Indrani, et al. "Improved magnetic and piezoresponse behavior of cobalt substituted BiFeO 3 thin film." *Thin Solid Films* 520.21 (2012): 6493-6498.

[41] Uniyal, Poonam, and K. L. Yadav. "Enhanced magnetoelectric properties in Bi 0.95 Ho 0.05 FeO 3 polycrystalline ceramics." *Journal of Alloys and Compounds* 511.1 (2012): 149-153.

[42] Yang, K. G., et al. "Structural, electrical, and magnetic properties of multiferroic Bi 1− x La x Fe 1− y Co y O 3 thin films." *Journal of Applied Physics* 107.12 (2010): 124109.

[43] Yan, Fuxue, et al. "In situ synthesis and characterization of fine-patterned La and Mn co-doped BiFeO 3 film." *Journal of Alloys and Compounds* 570 (2013): 19-22.

[44] Mao, Weiwei, et al. "Effect of Ln (Ln= La, Pr) and Co co-doped on the magnetic and ferroelectric properties of BiFeO 3 nanoparticles." *Journal of Alloys and Compounds* 584 (2014): 520-523.

[45] Singh, S. K., H. Ishiwara, and K. Maruyama. "Room temperature ferroelectric properties of Mn-substituted Bi Fe O 3 thin films deposited on Pt electrodes using chemical solution deposition." *Applied Physics Letters* 88.26 (2006): 262908.

[46] Kumar, Manoj, and K. L. Yadav. "Rapid liquid phase sintered Mn doped Bi Fe O 3 ceramics with enhanced polarization and weak magnetization." *Applied Physics Letters* 91.24 (2007): 242901.

[47] Huang, Ji-Zhou, et al. "Effect of Mn doping on electric and magnetic properties of BiFeO 3 thin films by chemical solution deposition." *Journal of Applied Physics* 106.6 (2009): 063911.

[48] Haumont, R., et al. "Effect of high pressure on multiferroic BiFeO 3." *Physical Review B* 79.18 (2009): 184110.

[49] Lebeugle, Delphine, et al. "Electric field switching of the magnetic anisotropy of a ferromagnetic layer exchange coupled to the multiferroic compound BiFeO 3." *Physical Review Letters* 103.25 (2009): 257601.

[50] Fruth, V., et al. "Preparation of BiFeO 3 films by wet chemical method and their characterization." *Journal of the European Ceramic Society* 27.2 (2007): 937-940.

[51] Cazayous, M., et al. "Possible observation of cycloidal electromagnons in BiFeO 3." *Physical review letters* 101.3 (2008): 037601.

[52] Lennox, Robert C., et al. "PZT-like structural phase transitions in the BiFeO 3–KNbO 3 solid solution." *Dalton Transactions* 44.23 (2015): 10608-10613.

[53] Lee, Seongsu, et al. "Single ferroelectric and chiral magnetic domain of single-crystalline BiFeO 3 in an electric field." *Physical Review B* 78.10 (2008): 100101.

[54] Kim, Jong Kuk, et al. "Enhanced ferroelectric properties of Cr-doped Bi Fe O 3 thin films grown by chemical solution deposition." *Applied physics letters* 88.13 (2006): 132901.

[55] Ghosh, Sushmita, et al. "Low-temperature synthesis of nanosized bismuth ferrite by soft chemical route." *Journal of the American Ceramic Society* 88.5 (2005): 1349-1352.

[56] Zhu, X. H., et al. "Thickness-dependent structural and electrical properties of multiferroic Mn-doped BiFeO 3 thin films grown epitaxially by pulsed laser deposition." *Applied Physics Letters* 93.8 (2008): 082902.

[57] Shibata, S., et al. "Preparation of silica microspheres containing Ag nanoparticles." *Journal of sol-gel science and technology* 11.3 (1998): 279-287.

[58] Hahn, Horst, P. Mondal, and K. A. Padmanabhan. "Plastic deformation of nanocrystalline materials." *Nanostructured materials* 9.1-8 (1997): 603-606.

[59]eresources.gitam.edu/nano/NANOTECHNOLOGY/role_of_bottomup_and_topdown_a.htm.

[60] Weinstein, Milton C., et al. "Principles of good practice for decision analytic modeling in health-care evaluation: report of the ISPOR Task Force on Good Research Practices—Modeling Studies." *Value in health* 6.1 (2003): 9-17.

[61] Jaeger, R.C., et al. "Film Deposition: Introduction to Microelectronic Fabrication, Upper Saddle Rivers, Prentice Hall, Rivers." (2002): 83.

[62] Park, Tae-Jin, et al. "Size-dependent magnetic properties of single-crystalline multiferroic BiFeO3 nanoparticles." *Nano letters* 7.3 (2007): 766-772.

[63] Jiang, Qing-Hui, Ce-Wen Nan, and Zhi-Jian Shen. "Synthesis and Properties of Multiferroic La-Modified BiFeO3 Ceramics." *Journal of the American Ceramic Society* 89.7 (2006): 2123-2127.

[64] Das, Nandini, et al. "Nanosized bismuth ferrite powder prepared through sonochemical and microemulsion techniques." *Materials Letters* 61.10 (2007): 2100-2104.

[65] Ghosh, Sushmita, et al. "Low temperature synthesis of bismuth ferrite nanoparticles by a ferrioxalate precursor method." *Materials research bulletin* 40.12 (2005): 2073-2079.

[66] Guo, Renqing, et al. "Enhanced photocatalytic activity and ferromagnetism in Gd doped BiFeO3 nanoparticles." *The Journal of Physical Chemistry C* 114.49 (2010): 21390-21396.

[67] "File: Sol-Gel Technology Scheme.png." *Wikimedia Commons, the free media repository*. 22 Jul 2014, 17:01

[68] Brinker, C. Jeffrey, and George W. Scherer. *Sol-gel science: the physics and chemistry of sol-gel processing*. Academic press, 2013.

[69] Hench, Larry L., and Jon K. West. "The sol-gel process." *Chemical reviews* 90.1 (1990): 33-72.

[70] Lopez, T., R. Gomez, and L. C. Klein. "Sol-Gel Optics: Processing and Applications." (1994): 345.

[71] Ezema, Fabian, and Rose Osuji. "A study of the optical properties of un-doped and potash doped lead chloride crystal in silica gel." (2012).

[72] Okpala, U. V., F. I. Ezema, and R. U. Osuji. "Synthesis and Characterization of Local Impurity Doped Stannous Iodide (SnI2) Crystal in Silica Gel." *Advances in in Applied Science Research* 3.2 (2012): 1174-1184.

[73] Ezema, Fabian, and Rose Osuji. "A study of the optical properties of un-doped and potash doped lead chloride crystal in silica gel." (2012).

[74] Meier, Michael AR, Richard Hoogenboom, and Ulrich S. Schubert. "Combinatorial methods, automated synthesis and high-throughput screening in polymer research: The evolution continues." *Macromolecular rapid communications* 25.1 (2004): 21-33.

[75] Wright, John D., and Nico AJM Sommerdijk. *Sol-gel materials: chemistry and applications*. Vol. 4. CRC press, 2000.

[76] Aegerter, Michel A., and Martin Mennig, eds. *Sol-gel technologies for glass producers and users*. Springer Science & Business Media, 2013.

[77] D'apuzzo, M., et al. "Sol-gel synthesis of humidity-sensitive P2O5-SiO2 amorphous films." *Journal of sol-gel science and technology* 17.3 (2000): 247-254.

[78] Brinker, C. Jeffrey, and George W. Scherer. *Sol-gel science: the physics and chemistry of sol-gel processing*. Academic press, 2013.

[79] Edwin, Berger, and Geffcken Walter. "Method for producing layers on solid objects." U.S. Patent No. 2,366,516. 2 Jan. 1945.

[80] Lopez, T., R. Gomez, and L. C. Klein. "Sol-Gel Optics: Processing and Applications." (1994): 345.

[81] Sakka, S., and K. Kamiya. "The sol-gel transition in the hydrolysis of metal alkoxides in relation to the formation of glass fibers and films." *Journal of Non-Crystalline Solids* 48.1 (1982): 31-46.

[82] Stoner, Eric J., et al. "Synthesis of HIV protease inhibitor ABT-378 (Lopinavir)." *Organic Process Research & Development* 4.4 (2000): 264-269.

[83] Schmidt, H. "Chemistry of material preparation by the sol-gel process." *Journal of Non-Crystalline Solids* 100.1-3 (1988): 51-64.

[84] Ward, David A., and Edmond I. Ko. "Preparing catalytic materials by the sol-gel method." *Industrial & engineering chemistry research* 34.2 (1995): 421-433.

[85] "File: ThermalCVD.PNG." *Wikimedia Commons, the free media repository*. 11 Apr 2015, 02:42

[86] Kim, Chan Soo, et al. "Direct measurement of nucleation and growth modes in titania nanoparticles generation by a CVD method." *Journal of chemical engineering of Japan* 37.11 (2004): 1379-1389.

[87] Sudarshan, T. S. "In Coated powders-new horizons and applications, Advances in Surface Treatment: Research & Applications (ASTRA)." *Proceedings of the International Conference, Hyderabad, India*. 2003.

[88] Carp, Oana, Carolien L. Huisman, and Armin Reller. "Photoinduced reactivity of titanium dioxide." *Progress in solid state chemistry* 32.1 (2004): 33-177.

[89] Xu, Feng, and Litao Sun. "Solution-derived ZnO nanostructures for photoanodes of dye-sensitized solar cells." *Energy & Environmental Science* 4.3 (2011): 818-841.

[90] "File: MBE.png." *Wikimedia Commons, the free media repository*. 16 Dec 2014, 19:51 UTC

[91] "File: Bragg XRD.svg." *Wikimedia Commons, the free media repository*. 25 Nov 2016, 02:22

[92] "File: Schematic SECOM text.jpg." *Wikimedia Commons, the free media repository*. 18 Jan 2017, 11:43

[93] wiringdiagram.online-ar.info/primiary-meter-wiring-diagram/

[94] www.radio-electronics.com/info/t_and_m/lcr-meter/basics-tutorial.php

[95] "File:FTIR Interferometer.png." *Wikimedia Commons, the free media repository*. 27 Mar 2015, 22:09

[96] "File:Schematic of UV- visible spectrophotometer.png." *Wikimedia Commons, the free media repository*. 24 Nov 2016, 17:19

[97] (a) Guo, Renqing, et al. "Enhanced photocatalytic activity and ferromagnetism in Gd doped BiFeO3 nanoparticles." *The Journal of Physical Chemistry C* 114.49 (2010): 21390-21396; (b) Khomchenko, V. A., et al. "Effect of Gd substitution on the crystal structure and multiferroic properties of BiFeO 3." *Acta Materialia* 57.17 (2009): 5137-5145.

[98] Guo, Renqing, et al. "Enhanced photocatalytic activity and ferromagnetism in Gd doped BiFeO3 nanoparticles." *The Journal of Physical Chemistry C* 114.49 (2010): 21390-21396.

[99] Mukherjee, A., et al. "Enhancement of multiferroic properties of nanocrystalline BiFeO 3 powder by Gd-doping." *Journal of Alloys and Compounds* 598 (2014): 142-150.

[100] (a) Lin, Yuan-Hua, et al. "Enhancement of ferromagnetic properties in Bi Fe O 3 polycrystalline ceramic by La doping." *Applied Physics Letters* 90.17 (2007): 172507. ; (b) Naik, V. B., and R. Mahendiran. "Magnetic and magnetoelectric studies in pure and cation doped." *Solid State Communications* 149.19 (2009): 754-758.

[101] Wang, Yao, and Ce-Wen Nan. "Site modification in Bi Fe O 3 thin films studied by Raman spectroscopy and piezoelectric force microscopy." *Journal of Applied Physics* 103.11 (2008): 114104.

[102] Reetu, et al. "Phase transformation, dielectric and magnetic properties of Nb doped Bi0. 8Sr0. 2FeO3 multiferroics." *Journal of Applied Physics* 111.11 (2012): 113917.

[103] Arya, G. S., R. K. Kotnala, and N. S. Negi. "Enhanced magnetic and magnetoelectric properties of In and Co codoped BiFeO3 nanoparticles at room temperature." *Journal of nanoparticle research* 16.1 (2014): 2155.

[104] Kumar, Manoj, and K. L. Yadav. "Rapid liquid phase sintered Mn doped Bi Fe O 3 ceramics with enhanced polarization and weak magnetization." *Applied Physics Letters* 91.24 (2007): 242901.

[105] Kalantari, Kambiz, et al. "Ti-Doping to Reduce Conductivity in Bi0. 85Nd0. 15FeO3 Ceramics." *Advanced Functional Materials* 21.19 (2011): 3737-3743.

[106] Park, Tae-Jin, et al. "Size-dependent magnetic properties of single-crystalline multiferroic BiFeO3 nanoparticles." *Nano letters* 7.3 (2007): 766-772.

[107] Sosnowska, I., T. Peterlin Neumaier, and E. Steichele. "Spiral magnetic ordering in bismuth ferrite." *Journal of Physics C: Solid State Physics* 15.23 (1982): 4835.

[108] Popov, Yu F., et al. "Linear magnetoelectric effect and phase transitions in bismuth ferrite BiFeO3." *ZhETF Pisma Redaktsiiu* 57 (1993): 65.

[109] Gautam, Ashish, et al. "Crystal structure and magnetic property of Nd doped BiFeO 3 nanocrytallites." *Materials Letters* 65.4 (2011): 591-594.

[110] Yan, Feng, et al. "Enhanced multiferroic properties and valence effect of Ru-doped BiFeO3 thin films." *The Journal of Physical Chemistry C* 114.15 (2010): 6994-6998.

[111] Park, Tae-Jin, et al. "Size-dependent magnetic properties of single-crystalline multiferroic BiFeO3 nanoparticles." *Nano letters* 7.3 (2007): 766-772.

[112] Mishra, R. K., et al. "Effect of yttrium on improvement of dielectric properties and magnetic switching behavior in BiFeO3." *Journal of Physics: Condensed Matter* 20.4 (2008): 045218.

[113] Rao, GV Subba, C. N. R. Rao, and J. R. Ferraro. "Infrared and electronic spectra of rare earth perovskites: ortho-chromites,-manganites and-ferrites." *Applied Spectroscopy* 24.4 (1970): 436-445.

[114] Chen, Chao, et al. "Hydrothermal synthesis of perovskite bismuth ferrite crystallites." *Journal of Crystal Growth* 291.1 (2006): 135-139.

[115] Xu, Jia-Huan, et al. "Low-temperature synthesis of BiFeO 3 nanopowders via a sol–gel method." *Journal of Alloys and Compounds* 472.1 (2009): 473-477.

[116] Ghosh, Sushmita, et al. "Low-temperature synthesis of nanosized bismuth ferrite by soft chemical route." *Journal of the American Ceramic Society* 88.5 (2005): 1349-1352.

[117] Zhang, Hongwu, et al. "Synthesis and luminescent properties of nanosized YVO 4: Ln (Ln= Sm, Dy)." *Journal of Alloys and Compounds* 457.1 (2008): 61-65.

[118] Nguyen, My H., Sang-Jin Lee, and Waltraud M. Kriven. "Synthesis of oxide powders by way of a polymeric steric entrapment precursor route." *Journal of materials research* 14.8 (1999): 3417-3426.